NASA TECHNICAL NOTE

NASA TN D-4127

NASA TN D-4127

HEAT- AND MASS-TRANSFER CHARACTERISTICS OF AN AXIAL-FLOW LIQUID-CORE NUCLEAR ROCKET EMPLOYING RADIATION HEAT TRANSFER

by Robert G. Ragsdale, Albert F. Kascak, and Leo F. Donovan

Lewis Research Center
Cleveland, Ohio

NATIONAL AERONAUTICS AND SPACE ADMINISTRATION • WASHINGTON, D. C. • AUGUST 1967

HEAT- AND MASS-TRANSFER CHARACTERISTICS OF AN AXIAL-FLOW LIQUID-CORE NUCLEAR ROCKET EMPLOYING RADIATION HEAT TRANSFER

By Robert G. Ragsdale, Albert F. Kascak, and Leo F. Donovan

Lewis Research Center
Cleveland, Ohio

NATIONAL AERONAUTICS AND SPACE ADMINISTRATION

For sale by the Clearinghouse for Federal Scientific and Technical Information
Springfield, Virginia 22151 – CFSTI price $3.00

HEAT- AND MASS-TRANSFER CHARACTERISTICS OF AN AXIAL-FLOW LIQUID-CORE NUCLEAR ROCKET EMPLOYING RADIATION HEAT TRANSFER

by Robert G. Ragsdale, Albert F. Kascak, and Leo F. Donovan

Lewis Research Center

SUMMARY

An analysis of heat- and mass-transfer processes was conducted for a liquid-core nuclear rocket engine that employs radiation heat transfer. A liquid carbide fuel was supported on the inside surface of a rotating tube. The hydrogen propellant, seeded with radiation-absorbing seed material, flowed through the tube where it was heated by thermal radiation from the fissioning liquid fuel. Liquid-fuel surface temperature, uranium concentration in the fuel, tube length and diameter, and hydrogen flow rate were the primary variables. Calculations were made for both zirconium carbide and niobium carbide solvents in which uranium carbide was dispersed.

The calculations show that radiant heating produces a specific impulse somewhere between the lowest value of interest, 1300 seconds, and the maximum attainable, about 1600 seconds - a value that is only marginally higher than that provided by conduction heating of hydrogen bubbled through the liquid fuel. The ratio of hydrogen flow rate to uranium flow rate is likely to range from about 20 to 100, depending on what compromises are chosen in flow-rate ratio, reactor pressure, tube diameter, and thrust to core-weight ratio. When the other parameters are within reasonable limits, the thrust to core-weight ratio is between 3 and 13. The surface temperature of the liquid fuel must be maintained between 9000° and $10\ 000^{\circ}$ R in order to attain a specific impulse in the range of interest. This requirement causes what is probably the major problem in designing a liquid-core nuclear rocket, that is, how to support a liquid fuel that is at a temperature higher than any known melting point. If a vapor film is not formed to insulate the solid structure from the liquid fuel, too large a fraction of the reactor power is conducted into the temperature-limited solid region of the reactor, and the specific impulse is reduced to solid-core levels.

INTRODUCTION

Nuclear rocket engines can be categorized by the physical state of the fissionable fuel or the fuel-bearing material (i. e., solid, liquid, or gas). Solid-core engines involve no drastic departure from the state-of-the-art heat-exchanger design, at least from a thermal design viewpoint, because the nuclear fuel is immobile, embedded within a solid fuel-element material. Performance of a solid-core engine is determined by the maximum temperature of the fuel element. In principle, a gaseous-fueled engine could raise the hydrogen propellant to temperatures considerably above the melting point of solid materials. Thus, gaseous reactors may attain a specific impulse of about 2500 seconds, compared with 800 seconds for a solid-core engine. Along with this performance advantage, however, gaseous-reactor designs introduce a number of complex interactions of fluid mechanics, heat transfer, and reactor criticality. Some recent studies of gaseous-reactor problems are described in reference 1.

Some of the complexity, and perhaps the level of performance, of a gaseous-fueled reactor can be reduced by maintaining the nuclear fuel as a liquid in the reactor. Such a liquid-core engine does not incur the complicated gas-core problems that result from fuel mobility. Since the heat source is a hot liquid rather than a radiating cloud of gas, a possible mode of operation is to bubble the cold hydrogen propellant radially inward through a liquid fuel layer that is suspended on the inner surface of a rotating tube. Such a system has been analytically assessed, both as a single cavity (ref. 2) and as a multi-unit tube bundle (ref. 3).

Up to a point, increased performance (higher specific impulse) can be obtained by operating the liquid-fuel region at higher temperatures. However, the vapor pressure of the liquid at higher temperatures, drives sufficient material into the hydrogen to increase the average propellant molecular weight enough to reduce the specific impulse. Therefore, there is an "optimum" liquid-fuel temperature that gives a maximum specific impulse. For the multitube engine, a specific impulse of 1500 seconds is calculated at a thrust to engine-weight ratio of the order of 1 (ref. 3). The fundamental limit on the specific impulse of this system derives from the fact that both heat and mass are transported into the gas by the same (conduction) process. Thus, a change of some parameter, such as bubble size or velocity, that leads to a reduction in mass transfer, correspondingly decreases heat transfer. An additional mechanism must be introduced to upset this balance in favor of heat transfer if the performance is to be improved.

It has been suggested that thermal radiation could be employed to transfer heat from the liquid fuel to the hydrogen (ref. 4). In such a system, the propellant would flow over the surface of the liquid rather than bubble through it. If the surface temperature were high enough, the energy transport would be primarily by radiation, and mass transfer effectiveness would be less than that of heat transfer. However, there are some imme-

diately obvious disadvantages that may limit or offset the potential gain of this flow pattern. The liquid surface temperature must be higher than the desired propellant exhaust temperature; in the bubble-through system, the two temperatures are equal. Also, the liquid-fuel temperature must be high enough for radiative transfer to dominate; otherwise, the mass-transfer - heat-transfer analogy would still hold. These factors could lead to (1) substantial loss of heavy vapor even though the mass-transfer effectiveness is low, and (2) excessive heat conduction radially outward into the solid structure. An inherent advantage of the thermal-radiation system is that engine thrust is not limited by rotational speed as it is in the bubble-through system.

Two difficulties involved in evaluating this engine concept deserve mention: first, there is an impractically large number of independent variables; and, second, some of the required input information is not available. The number of variables was reduced by assigning fixed or limiting values to the following items: fuel material, uranium carbide; seeded hydrogen opacity, 3; and hydrogen temperature at the inlet to the fuel passage, 3500° R. Most of the parametric calculations were performed for a reactor pressure of 100 atmospheres; although some cases were performed for 500 atmospheres, and a final, sample case was computed for a pressure of 200 atmospheres. Zirconium carbide and niobium carbide were the two fuel solvents considered. Three values each were taken for fuel surface temperature, tube diameter and length, uranium carbide mole fraction in the fuel, and hydrogen mass velocity. The most significant information not available is the vapor pressure of the elements and compounds that make up the liquid fuel. These values were obtained by extrapolating information presented in references 5 to 10. It was also assumed that the composition of the vapor in equilibrium with the liquid fuel could be determined by applying Raoult's law directly to the molecular constituents of the fuel, although the actual behavior of such a ternary system is undoubtedly more complex (ref. 11). Radiant heat transfer was computed by using techniques described in references 12 and 13. Mass-transfer calculations were made by using the mass-transfer - heat-transfer analogy as described in reference 14.

This analysis was performed to assess some of the heat- and mass-transfer characteristics of a liquid-core nuclear engine in which thermal radiation is the primary mode of heat transfer. Calculations were made to determine outlet gas temperature, exhaust gas composition, and specific impulse. The uranium loss rate, presented as the ratio of hydrogen flow rate to uranium flow rate, was determined for various uranium concentrations in the liquid fuel and for various fuel surface temperatures. An estimate was made of engine thrust to core-weight ratio for a particular set of conditions. Although the foregoing approximations and extrapolations introduce some uncertainties into the calculations, it is felt that sufficient accuracy remains for the purpose of this study; that is, to determine the performance advantage of such a system in terms of specific impulse or thrust to weight ratio over a bubble-through flow configuration.

ANALYSIS

The basic model, physical and chemical properties, and equations used to calculate the heat- and mass-transfer characteristics of a radiation-heat-transfer liquid-core nuclear rocket are presented in this section. First, the model of the reactor flow passage is described. Next, the engine cycle is discussed with regard to an overall energy balance. Finally, the equations used to calculate heat-transfer, mass-transfer, and engine performance parameters are presented.

Model for Calculation

A schematic view of the reactor flow passage is shown in figure 1(a). As the hydrogen flows axially through the rotating tube, two processes occur: first, the hydrogen absorbs heat that is radiated from the inner surface of the liquid fuel; and second, because the liquid exerts a significant vapor pressure, uranium carbide and metallic carbide molecules diffuse into the flowing hydrogen and are carried from the tube. The tube rotation simply provides sufficient body force to hold the liquid fuel on the solid liner. A bubble-through system is similar, except that the hydrogen enters through the cylindrical solid wall, bubbles through the liquid fuel, and then flows axially down the tube.

The calculations primarily involve heat and mass transfer to a gas flowing in a tube with a fully developed turbulent-velocity profile. It is assumed that the two processes do not affect each other, except insofar as the liquid surface (boundary) temperature T_s also determines the concentration of the carbide species at the wall through the vapor-pressure curves of the fuel constituents. Figure 1(b) shows the model used for the calculations. A given mass flow rate of hydrogen, at reactor pressure P_R, flows through a tube of specified dimensions. The propellant properties, specific heat c_p, viscosity μ, and opacity τ (product of absorption coefficient and tube diameter), are known and assumed to be constant. Thermal radiation is emitted from the inner surface of the liquid, which is at some constant temperature T_s. Mass diffuses into the flowing hydrogen stream from the constant mass fraction boundary C_s. The composition of the carbide vapor at the wall is calculated from the vapor pressure of the pure compounds at T_s and Raoult's law, which relates the vapor composition to the composition of the liquid. Pure hydrogen enters the tube at some inlet temperature T_1. The same flow rate of hydrogen, along with some additional flow rate of carbide vapor, exits from the tube at some higher temperature T_2.

The specific impulse attainable with pure hydrogen is shown in figure 2 for reactor pressures of 100, 250, and 500 atmospheres. These curves were calculated from enthalpy values reported in reference 15. All the kinetic energy of the hydrogen does

not produce thrust because of nonequilibrium expansion and a finite nozzle area ratio. The specific impulse shown in figure 2 was calculated by arbitrarily assuming a value of 0.9 for a nozzle coefficient (i.e., 81 percent of the propellant enthalpy is converted into thrust). This assumption is probably optimistic.

If any part of the reactor power is transferred to the hydrogen in a solid, temperature-limited region, there is a maximum specific impulse that can be obtained. This requirement of an overall energy balance on the engine, which has been shown by a number of authors, is illustrated in figure 3. This limitation could be significant in a liquid-core engine if an excessive amount of heat is conducted radially outward into the solid structure of the engine. For example, if 25 percent of the reactor power is deposited in the hydrogen at 3600° R, 1430 seconds is the maximum impulse obtainable.

Heat Transfer

Radiation. - The radiant heat exchange between the liquid surface and the axially flowing propellant gas was computed by a computer program described in reference 13. The program represents a numerical solution of the radiative transport equation. The output of the program is gas temperature profiles, both radial and axial.

A number of assumptions are involved, but none represents any serious limitation for the situation of interest here. The gas is assumed to be gray; that is, the absorption coefficient is independent of wavelength. Since most or all the hydrogen opacity results from the addition of a solid-particle seed material, no strong dependence of absorption coefficient on wavelength is likely. The gas is assumed to be in local thermodynamic equilibrium; therefore, the emissive power can be calculated by using an absorption coefficient. The walls are assumed to be black. The program requires that velocity profiles be specified; slug flow is assumed for all cases calculated. Viscous dissipation and conduction are assumed to have negligible effects on energy transport. Finally, scattering is neglected; emitted radiant energy is either absorbed or transmitted.

The use of these assumptions results in an energy equation with four terms: a convective term proportional to the axial gradient of temperature; an emission term proportional to the fourth power of temperature; and two absorption terms proportional to the fourth power of some mean local temperature. The last two terms represent energy radiated into a gas volume element from surrounding elements and from the boundary surfaces. The energy equation is

$$-\rho v c_p \frac{\partial T_f}{\partial z} - 4k_f \sigma T_f^4 + k_f \int_V \frac{4k_e \sigma T_e^4}{4\pi R^2} e^{-\tau} dV + k_f \int_S \frac{\sigma T_s^4}{\pi R^2} e^{-\tau_s} (\hat{r} \cdot \hat{n}) ds = 0 \qquad (1)$$

where $\hat{r}$ and $\hat{n}$ are unit direction vectors. (All symbols are defined in the appendix.)

The program provides an iterative numerical solution to equation (1). The program output is $T(r,z)$, as well as integrated values of bulk gas temperature. An initial temperature distribution is assumed, the mean local temperature is evaluated, and then a new temperature distribution is obtained by solving equation (1). This process is repeated until temperature distributions on two successive iterations change by less than some specified amount.

Program input requires values for an absorption coefficient, mass velocity, specific heat, tube diameter, tube length, initial gas temperature, and tube wall temperature. For all the calculations in this study, the gas inlet temperature was taken to be 3500° R and specific heat to be 6 Btu per pound per $^{\circ}$R.

The two integral terms in equation (1) are significant; they describe the effectiveness with which energy is transported from the wall into a given volume element of gas. If there were no geometric view factors and if every volume of gas were to receive unattenuated radiant flux, the wall and the gas would simply interchange heat as blackbodies. For this situation, the energy equation becomes

$$4\left(\frac{L}{D}\right)\sigma\left(T_s^4 - T_b^4\right) = \rho v c_p \frac{dT_b}{d\left(\frac{z}{L}\right)} \tag{2}$$

Equation (2) gives the variation of the bulk gas temperature T_b with tube length L for the case of "perfect" coupling between the heat source and the heat sink. A comparison of equations (1) and (2) indicates how much the heat-transfer rate into the gas has been reduced by the view factors. Obviously, T_f from equation (1) is always equal to or less than T_b from equation (2). The maximum rate of heat deposition would occur if there were no back radiation from the gas to the wall; such a situation is described by deleting the T_b^4 term from equation (2).

Conduction. - The internal temperature distribution in the liquid fuel and surrounding solid structure can be calculated for specified boundary conditions, dimensions, and thermal conductivities. In cylindrical coordinates, the energy equation for conduction and internal heat generation is

$$\frac{1}{r}\frac{d}{dr}\left(k_l r \frac{dT}{dr}\right) + q'''(r) = 0 \tag{3}$$

For a thermal conductivity that is independent of temperature, equation (3) can be partially integrated to give

$$\frac{dT}{dr} = -\frac{1}{r}\int_{r_s}^{r} \frac{r}{k\ell}\, q'''(r)dr + \frac{r_s}{r}\frac{dT}{dr}\bigg|_{r=r_s} \tag{4}$$

where r_s is the radius of the liquid surface and $(dT/dr)_{r=r_s}$ is the temperature gradient in the liquid fuel at the surface. This gradient is determined for a given net heat flux leaving the liquid surface.

Equation (4) can be integrated to give the temperature distribution in the liquid fuel region $T(r)$ by using the known surface temperature T_s as a boundary value:

$$T = -\int_{r_s}^{r} \frac{1}{r}\int_{r_s}^{r} \frac{r}{k\ell}\, q'''(r)dr\, dr + r_s\left(\frac{dT}{dr}\right)_{r=r_s} \ln\frac{r}{r_s} + T_s \tag{5}$$

The volumetric heat-generation rate q''' is determined by two quantities: (1) the net heat radiated from the liquid surface into the flowing gas and (2) the additional amount of heat that is conducted radially outward from the liquid fuel region into the surrounding structure. If r_{int} is the outer radius of the liquid fuel annulus, ψ is the fraction of reactor power that "leaks" out into the solid structure, and ϵ is an effective emissivity of the liquid surface, a heat balance gives

$$2\pi r_s \epsilon\sigma T_s^4 = (1 - \psi)\int_{r_s}^{r_{int}} 2\pi r q'''(r)dr \tag{6}$$

The term ϵ accounts both for the actual emissivity of the surface and for the reduction in net heat flow due to back radiation from the gas; it is obtained from the calculated net heat transfer to the flowing propellant gas.

The volumetric heat-generation rate is assumed to be constant, as it would be for uniform fuel dispersion and no flux depression. Integrating and combining equations (5) and (6) give the temperature distribution through the fuel region as

$$T = T_s + \frac{r_s}{k_\ell}\epsilon\sigma T_s^4 \ln\frac{r}{r_s} - \frac{r_s}{k_\ell}\epsilon\sigma T_s^4 \frac{1}{(1 - \psi)\left(r_{int}^2 - r_s^2\right)}\left(\frac{r^2 - r_s^2}{2} - r_s^2 \ln\frac{r}{r_s}\right) \tag{7}$$

For the solid region beyond r_{int} there is no internal heat generation, the thermal

conductivity is that of the solid k_C, and the heat flow is ψ times the total reactor power generation. The temperature profile in this region is given by

$$T(r) = T_{int} = \frac{r_s}{k_C} \frac{\psi \epsilon \sigma T_s^4}{(1 - \psi)} \ln \frac{r}{r_{int}} \tag{8}$$

Mass-Transfer Calculations

Some of the liquid contained on the tube wall vaporizes and is carried out with the exhaust. The following analysis determines the outlet-bulk mass fraction of uranium carbide (UC_2) with either niobium carbide (NbC) or zirconium carbide (ZrC) from which uranium loss rates and specific impulse degradation can be estimated.

For mass-transfer calculations, it is assumed that the rotation of the tube causes the liquid layer to be uniformly distributed along the tube wall. The flow geometry is then a cylinder with a radius equal to the tube radius minus the liquid layer thickness. The vapor at the liquid-vapor interface is in equilibrium with the liquid. Therefore, the vapor composition can be calculated approximately from Raoult's law, which states that the equilibrium vapor pressure that is exerted by a component in a solution P_i is proportional to the mole fraction of that component X_i, that is,

$$P_i = X_i P_i^o \tag{9}$$

where P_i^o is the vapor pressure of a component i in the pure state. It is further assumed that the composition and temperature of the liquid are constant along the tube and do not change with time. Therefore, the composition of the vapor at the interface will be constant.

For the range of conditions covered in the calculations, Reynolds numbers varied from 12 000 to 120 000, and tube length to diameter ratios ranged from 15 to 30. Therefore, all mass-transfer calculations were made on the basis of fully developed turbulent flow.

Since radial concentration gradients of UC_2 and ZrC or NbC exist, there is also a corresponding radial gradient of hydrogen concentration. This concentration gradient causes a diffusive flux of hydrogen toward the liquid surface. The surface is assumed to be impermeable to hydrogen; thus, a convective flow of carbide vapor of equal magnitude but opposite in direction is set up. This convective flow away from the liquid surface causes an additional transport of carbide species over and above the diffusive transport.

This effect is included in the mass-transfer calculations, but it is never the dominant mode of transfer.

The importance of the convective velocity can be estimated from the magnitude of the mass-transfer parameter:

$$B = \frac{\left(y_{UC_2,\,s} + y_{XC,\,s}\right) - \left(y_{UC_2,\,b} + y_{XC,\,b}\right)}{1 - \left(y_{UC_2,\,s} + y_{XC,\,s}\right)} \tag{10}$$

where y is mole fraction in the vapor, and the subscripts s and b indicate surface and bulk, respectively. When B is less than 1, the convective velocity can be ignored and the heat-transfer - mass-transfer analogy can be used to determine the mass-transfer coefficient. Thus, if the friction factor is known, the mass-transfer coefficient can be calculated from the j-factor relation, $j = f/2$. For a Schmidt number of 1, the j-factor is

$$j = \frac{h_{do} M_{H_2}}{G} \tag{11}$$

where h_{do} is the mass-transfer coefficient at negligible mass-transfer rates. Reference 14 presents a plot of the j-factor as a function of Reynolds number.

When the mass-transfer rate is large, the effect of the convective velocity cannot be neglected. The solution to the mass-transfer problem can be obtained, however, by modifying the solution to the heat-transfer problem, that is, by using the film theory result discussed in reference 14. The ratio of the actual mass-transfer coefficient to that at negligible mass-transfer rates is given by

$$\frac{h_d}{h_{do}} \equiv \theta = \frac{\ln(1 + B)}{B} \tag{12}$$

The ratio of bulk mole fraction to surface mole fraction of UC_2 can be determined from a balance that equates the change in moles of UC_2 over an increment of length $\left(G/M_{H_2}\right)(\pi D^2/4)\Delta y_{UC_2,\,b}$ to the UC_2 transferred from the liquid surface in that length $N_{UC_2}\Delta z \pi D$. In differential form, this relation is

$$\frac{dy_{UC_2,\,b}}{dz} = \frac{4 M_{H_2} N_{UC_2}}{GD} \tag{13}$$

For the i^{th} component of a multicomponent mixture, the mass-transfer coefficient h_d can be defined as (ref. 14)

$$N_i - y_{i,s}\sum_j N_j = h_d(y_{i,s} - y_{i,b}) \tag{14}$$

Since the flux of hydrogen is zero at the liquid surface,

$$\sum_j N_j = N_{UC_2} + N_{XC} = -h_d\left(1 - \frac{y_{H_2,b}}{y_{H_2,s}}\right) \tag{15}$$

where N_{XC} is the surface molar flux of NbC or ZrC. The flux of UC_2 is thus

$$N_{UC_2} = h_d y_{UC_2,s}\left(\frac{y_{H_2,b}}{y_{H_2,s}} - \frac{y_{UC_2,b}}{y_{UC_2,s}}\right) \tag{16}$$

Equation (13) may then be written in the form

$$\frac{dy_{UC_2,b}}{y_{UC_2,s}\left(\frac{y_{H_2,b}}{y_{H_2,s}}\right) - y_{UC_2,b}} = 4j\theta\, d\,\frac{z}{D} \tag{17}$$

Integrating from the inlet, where the bulk mole fraction of UC_2 is zero, to any distance z gives

$$\frac{y_{UC_2,b}}{y_{UC_2,s}} = \frac{y_{H_2,b}}{y_{H_2,s}}\left(1 - e^{-4j\theta(z/D)}\right) \tag{18}$$

In a similar manner, for the metal carbide solvent

$$\frac{y_{XC,b}}{y_{XC,s}} = \frac{y_{H_2,b}}{y_{H_2,s}}\left(1 - e^{-4j\theta(z/D)}\right) \tag{19}$$

With the bulk- to surface-mole-fraction ratios known, it is possible to calculate mass fraction ratios. Some algebraic manipulation leads to

$$\frac{C_{UC_2,b}}{C_{UC_2,s}} = \frac{1}{1 + C_{H_2,s}\left(e^{4j\theta(z/D)} - 1\right)^{-1}} \tag{20a}$$

for uranium carbide mass fraction ratio. For hydrogen,

$$\frac{C_{H_2,b}}{C_{UC_2,b}} = \frac{C_{H_2,s}}{C_{UC_2,s}} \frac{1}{1 - e^{-4j\theta(z/D)}} \tag{20b}$$

The bulk mass fraction of the solvent XC (either ZrC or NbC) is then obtained by

$$C_{XC,b} = 1 - C_{UC_2,b} - C_{H_2,b} \tag{20c}$$

The ratio of hydrogen to uranium carbide mass fractions at the wall varied from 8 to 1.7 for wall temperatures from 9000° to $10\,000^{\circ}$ R. For a mass velocity of 10 pounds per second per square foot of hydrogen in a 4-inch-diameter tube, the Reynolds number was 120 000, and $j = 0.0022$. The θ correction was 1 for a NbC solvent and varied from 0.95 to 1.0 for ZrC. Equation (20b) was multiplied by the molecular weight ratio of UC_2 to U to obtain the weight ratio of hydrogen to uranium exiting the tube. Radial concentration profiles presented for the sample engine were obtained by assuming that they followed a 1/7 power variation with radius, similar to velocity profiles.

Engine Performance

The engine performance parameters of interest are thrust, specific impulse, weight, and fuel loss rate. The reactor core weight is readily calculated for a specific geometry and materials. The specific impulse of the propellant mixture is less than that of pure hydrogen at the same temperature because of the presence of high-molecular-weight species. The actual specific impulse can be obtained from

$$I_{sp} = \alpha_i I^*_{sp} \tag{21}$$

The correction factor α_i that is applied to the specific impulse of pure hydrogen I_{sp}^* is obtained by assuming that specific heat is inversely proportional to molecular weight. Thus, in terms of the propellant average molecular weight $\overline{M}$ and hydrogen molecular weight, assumed to be constant at 2, α_i is given by

$$\alpha_i = \sqrt{\frac{2}{\overline{M}}} \tag{22}$$

For a given bulk concentration of heavy component i, equation (22) becomes

$$\alpha_i = \sqrt{1 - \left(1 - \frac{2}{\overline{M}}\right) C_b} \tag{23}$$

For a specified hydrogen flow rate, the total propellant flow rate is

$$\dot{w}_p = \dot{w}_{H_2}\left(1 + \frac{C_b}{1 - C_b}\right) \tag{24}$$

The bulk mass fraction C_b is calculated from equation (20) for each of the components. The engine thrust is given by the product of propellant mass flow rate and specific impulse:

$$F = \dot{w}_p I_{sp} \tag{25}$$

RESULTS AND DISCUSSION

The results of this study fall into two categories: (1) a parametric series of engine performance calculations and (2) a more detailed calculation of a sample engine configuration selected on the basis of the parametric results.

Table I lists the values of the primary variables and also the combination of variables chosen for the sample engine calculation. Uranium carbide was used as the fissionable material; calculations were performed with both niobium carbide and zirconium carbide as solvents. Based on an initial variation, the hydrogen opacity τ (product of absorption coefficient K and tube diameter D) is assumed to have a constant value of 3. The propellant average specific heat and viscosity are assumed to be 6 Btu per pound per ^{o}F and 275×10^{-7} pound per foot per second (ref. 15), respectively. The temperature of the hy-

TABLE I. - VALUES OF PRIMARY INDEPENDENT VARIABLES

USED IN CALCULATIONS

Mole fraction uranium carbide in fuel, X_{UC_2}	Fuel surface temperature, T_s, ^oR	Hydrogen mass velocity, G_{H_2}, lb/(ft^2)(sec)	Tube diameter, D, in.	Tube length, L, ft	Reactor pressure, P_r, atm
0.002	9 000	1	4	5	100
.01	9 500	3	6	10	250
.05	10 000	10	8	15	500
[a].02	9 500	6.7	4	6.7	200

[a]Values selected for sample engine.

drogen entering the liquid fuel-element flow passage is assumed to be 3500^o R for all cases. Most of the parametric calculations are for a reactor pressure of 100 atmospheres; a few cases are also presented for 500 atmospheres to illustrate the effect of pressure level. The sample calculation is for a reactor pressure of 200 atmospheres.

Results are presented first showing the vapor composition at the surface of the liquid fuel. Next, outlet propellant temperatures are presented for the various flow rates, tube dimensions, and surface temperatures considered. Mass-transfer results are presented in terms of uranium to hydrogen mass fractions normalized to the saturation value at the liquid surface. The heat- and mass-transfer results are then presented in the form of specific impulse and fuel loss rate. Finally, sample engine parameters are selected from the parameter matrix studied, and detailed results for concentration profiles, temperature profiles, and fuel consumption rates are presented, as well as an estimate of reactor-core weight.

Fuel Vapor Composition

The equilibrium vapor composition over a liquid of specified mixture is readily estimated from equation (9) and the vapor pressures of the pure components. Figure 4 shows the vapor pressure curves used. The elemental curves for uranium and carbon are taken from reference 5. The uranium carbide curve is from reference 7. The ZrC curve is from reference 9, and the NbC curve is from reference 6. The curves were extended to pressures above 1 atmosphere by extrapolating them as straight lines. There is some indication (ref. 10) that the vapor pressure of niobium carbide may be higher than that shown in figure 4. The curve used there is the lowest reported value (ref. 6) and should therefore give a minimum fuel evaporation rate. The highest reported vapor pressure of NbC is still less than the curve used in figure 4 for ZrC; thus, the evapora-

ation rates obtained with the NbC and ZrC curves should bracket any more accurate answer based on better vapor pressure information. In the temperature range to be considered, from 9000° to 10 000° R, the extrapolated vapor pressure of ZrC is from 25 to 30 times that of NbC.

The vapor pressure of the pure compounds, the concentrations in the liquid phase, and Raoult's law give the composition of the heavy vapor in equilibrium with the liquid. Figure 5(a) shows that for a NbC solvent, the vapor is much richer in UC_2 than the liquid. The vapor composition is quite insensitive to temperature level in this range, which is a numerical result of the vapor pressure curves of NbC and UC_2 in figure 4 being parallel. Because of the different concentrations of UC_2 in the vapor and liquid phases, the concentration of UC_2 in the remaining liquid decreases with time. For example, consider an original mole fraction of UC_2 of 0.02 in the liquid fuel. After 1.7 atomic percent of the liquid has evaporated, 50 percent of the UC_2 has been lost. Thus, even if a relatively small amount of liquid fuel is consumed, it may be necessary during engine operation to replace the fissionable species as it evaporates from the liquid.

Figure 5(b) shows that the relative concentration of UC_2 in the heavy vapor is less for a ZrC solvent than for a NbC solvent, because ZrC has a higher vapor pressure than NbC and thus exerts a higher partial pressure. The UC_2, of course, exerts the same partial pressure for a given concentration in the liquid phase regardless of the solvent or its characteristics. Figure 5(b) also indicates that, at increased temperatures, the vapor is less rich in UC_2.

Figure 6 shows the average molecular weight of the heavy vapor as a function of the UC_2 concentration in the liquid, and the temperature for both ZrC and NbC solvents. The average molecular weight is insensitive to temperature because the vapor-pressure curves are nearly parallel, so that the relative composition of the vapor is essentially constant. The average molecular weight of the NbC/UC_2 mixture is greater than that of ZrC/UC_2 because of a higher proportion of UC_2 in the first mixture.

Although the heavy vapor represents only a small fraction of the total atoms present in the gas mixture at the liquid surface, it constitutes a substantial mass fraction because of its high molecular weight. Figure 7(a) shows the mass fraction of heavy vapor at the liquid surface for various temperatures, reactor pressures (sum of partial pressures), and liquid concentrations of UC_2 in NbC. The hydrogen density was calculated by using a molecular weight of 2; no dissociation is assumed for this calculation. The mass fractions are quite significant for a reactor pressure of 100 atmospheres; for example, for a liquid mole fraction of UC_2 of 0.02, heavy vapor mass fractions range from 0.125 at 9000° R to 0.39 at 10 000° R. The curves increase with increasing UC_2 concentration because UC_2 has a higher vapor pressure and a higher molecular weight than NbC. Figure 7(b) shows similar results for a ZrC solvent at a reactor pressure of 100 atmospheres. The mass fractions at the wall for ZrC are higher than for NbC and do not decrease appre-

ciably for small concentrations of UC_2 in the liquid because of the dominance of ZrC. Figure 7 is used to give the wall-concentration boundary values for mass-transfer calculations.

Heat Transfer

It is necessary to specify the absorption coefficient of the gas in order to calculate the radiant heat transfer to the flowing gas from the hot surface. This specification is normally done in terms of gas opacity τ which is the product of the absorption coefficient and the tube diameter. Opacity is, therefore, an optical dimension of the gas system. For a cylinder, the opacity is equivalent to the tube diameter expressed in terms of radiation mean free paths. It is shown in reference 12 that there is an optimum opacity that results in maximum heat transfer to the gas for the flow system considered here. If the gas is too transparent, the hot wall radiates to the opposite wall rather than to the gas; if the gas is too opaque, the radiation does not penetrate to the central, innermost regions of the gas. Figure 8(a) illustrates this effect of gas opacity on the bulk outlet gas temperature for the conditions of interest here. For maximum heat transfer to the gas, the absorption coefficient should be such that the tube is 2 to 4 mean free paths in diameter. All the heat-transfer calculations for this study were done for an opacity of 3.

The results of figure 8(a) are for an opacity corresponding to an absorption coefficient that is constant with radial position. The net amount of heat flow into the gas can be increased by causing the absorption coefficient to increase monotonically with radial distance from the wall. This increase could be accomplished by initially injecting more seed material along the tube centerline than near the wall. The maximum rate of net heat transfer to the gas can be obtained by using the transparent gas model in which it is assumed that the wall and the gas exchange radiation as though they were blackbodies at the surface and bulk temperatures, respectively.

Figure 8(b) shows a comparison of heat-transfer rates for three opacity assumptions. The upper curve, for no back radiation, could not be achieved in practice; it is included simply to help indicate the effect of back radiation. The fact that the middle curve is only slightly higher than the lower one indicates that no great gain is available from preferential seeding compared with a radially uniform distribution of seed material in the propellant. At most, the outlet gas temperature could be increased 500° R, or, for the same outlet temperature, the tube length could be decreased 15 percent.

The amount of seed material to be added to the hydrogen to achieve an opacity of 3 must be determined. Reference 16 reports some recent work on optical properties of small particles and provides a reference guide to other related studies. Based on these

experimental and analytical findings, it seems likely that absorption cross sections in the range from 10 000 to 20 000 square centimeters per gram are obtainable.

Figure 9 shows the amount of carbon that must be added to hydrogen at 100 atmospheres and 500° R to give an opacity of 3. For this analysis, hydrogen density was calculated from the perfect gas law, with no dissociation assumed. The results are shown as the mass fraction of carbon in hydrogen for various tube diameters. The curves for absorption cross sections of 4000 and 40 000 square centimeters per gram are considered realistic upper and lower limits for carbon particle seeds.

The significant aspect of the requirement to seed the hydrogen is that it places a lower limit on tube diameter. As shown in figure 9, smaller diameter tubes require greater mass fractions of seed material. The penalty of seed addition is the same as that of the fuel vapor; it decreases the specific impulse of the propellant by increasing its average molecular weight. The magnitude of this effect is shown in figure 10. For carbon contents from 10 to 20 weight percent in hydrogen, the specific impulse is decreased by about 5 to 10 percent, respectively.

From the information in figures 9 and 10, it does not appear likely that adding a particulate seed to the hydrogen to make it opaque will seriously penalize engine performance by causing a reduction in specific impulse. For example, if an absorption cross section of 40 000 square centimeters per gram can be obtained, a 1-inch-diameter tube would require a mass fraction of 0.05 in 100 atmospheres of hydrogen. This much seed would cause a 2-percent reduction in specific impulse.

A significant contributor to propellant opacity may be the heavy vapor evolved at the surface of the liquid lining the tube wall. If this is the case, estimates of heat transfer based on a radially constant absorption coefficient could be in error. The presence of a radiation boundary layer of physically thin, optically thick gas could greatly reduce the heat-transfer rate to the gas because of the self-shielding that would occur.

Some calculations were performed to assess the importance of this situation. It was assumed that the absorption coefficient was proportional to concentration and that, for fully developed turbulent flow, the concentration profile was given by a 1/7 power variation with radius. The heat-transfer rate for this case was compared with the constant absorption coefficient situation as shown in figure 11. The opacity (integrated optical diameter of the tube) τ is 3 for both case 1 and case 2. Figure 11(b) shows that thermal self-shielding when the average opacity is not much greater than 3 results in outlet gas temperatures that are only moderately (500° F) less than predictions based on a radially constant absorption coefficient. All the parametric calculations are based on a constant absorption coefficient.

Figure 12 shows the basic heat-transfer curves used in this study; they were calculated from equation (1) with a constant opacity of 3. Outlet gas temperature is given as a function of tube length to diameter ratio for three wall temperatures and three flow

rates. The same information is replotted in figure 13 for specific tube diameters of 4, 6, and 8 inches.

Mass Transfer

The rate at which the uranium carbide and the solvent carbide contaminate the hydrogen as it flows down the tube is illustrated in figure 14 for a 4-inch-diameter tube and a surface temperature of 10 000° R. The hydrogen mass velocity is 10 pounds per second per square foot, and the total reactor pressure is 100 atmospheres. Mass fractions in the bulk stream were calculated from equation (20). These results were used, along with the local bulk temperatures given in figure 12, to obtain the absolute density of each species shown in figure 14.

The UC_2 density is independent of the solvent, since it is determined only by its vapor pressure at the wall. The hydrogen density is essentially independent of the solvent; for the ZrC system shown in figure 14, the hydrogen partial pressure at a tube length of 20 feet is 96.4 atmospheres (of a total of 100 atm). The marked difference in the bulk density of ZrC and NbC in figure 14 is a direct consequence of their vapor pressures (fig. 4). These results indicate that in a ZrC/UC_2 system it is the ZrC that penalizes the specific impulse, but in a NbC/UC_2 system, it is the UC_2. Similar calculations were performed for wall temperatures of 9000° and 9500° R.

Engine Performance

Specific impulse. - Engine performance is discussed in terms of two criteria: attainable specific impulse and fuel loss rate. The specific impulse obtainable by radiatively heating pure hydrogen at 100 atmospheres is shown in figure 15 for a hydrogen mass velocity of 10 pounds per square foot per second. The specific impulse is given for a tube diameter of 4 inches at surface temperatures of 9000°, 9500°, and 10 000° R and for tube diameters of 6 and 8 inches at a surface temperature of 9500° R.

Figure 15 quantitatively illustrates two important features of the engine. One feature is that surface temperature is extremely important; for a 4-inch-diameter tube that is 10 feet long, surface temperatures of 9000°, 9500°, and 10 000° R lead to specific impulses of 1300, 1480, and 1660 seconds, respectively. Of course, these are maximum impulses; actual values are lowered by the presence of heavy vapor in the hydrogen. The second indication in figure 15 is that tube diameters much greater than 4 inches result in engines that are rather long, and therefore perhaps too heavy. For

this reason, the remaining curves of engine performance parameters are for a tube diameter of 4 inches.

Figure 16 illustrates the variation of specific impulse with tube length for three situations: pure hydrogen, and the NbC and ZrC systems. As tube length increases, the specific impulse for pure hydrogen approaches the value given in figure 2 at a temperature of 10 000° R, 1860 seconds. Curves for both the NbC and ZrC systems exhibit a maximum specific impulse, just as reported for the bubble-through reactor (refs. 2, 3, and 17). The reason for this maximum impulse is that higher wall temperatures increase the fuel vapor pressure, and therefore increase the amount of heavy vapor in the exhaust propellant. The NbC curve has a maximum specific impulse of about 1630 seconds at a tube length of about 16 feet. For longer tubes, the impulse decreases toward 1460 seconds, the specific impulse corresponding to a saturated propellant at 10 000° R and 100 atmospheres. If ZrC is used as a fuel diluent, the maximum specific impulse at 10 000° R is 1140 seconds, and the saturation limit is 790 seconds.

Although the curves of figure 16 are for a particular wall temperature of 10 000° R, they exhibit two general characteristics of this kind of flow passage. First, there is an optimum tube length that gives a maximum impulse, and, second, the maximum specific impulse is higher for the NbC system than for the ZrC system, predicated on the validity of the vapor-pressure curves used.

Figure 17 shows the effect of surface temperature on specific impulse for NbC and ZrC diluents. The maximum specific impulse for NbC decreases with decreasing tube wall temperature (fig. 17(a)). For ZrC, both the maximum specific impulse and the optimum tube length are affected by varying the surface temperature from 9000° to 10 000° R (fig. 17(b)).

The results shown in figure 17 indicate the specific impulses available from a liquid-fueled reactor operating at a pressure of 100 atmospheres with a UC_2 mole fraction of 0.02 in the fuel. With a NbC solvent, a specific impulse ranging from about 1500 to 1600 seconds can be obtained with fuel surface temperature in the range from 9000° to 10 000° R. Higher impulses are probably not possible since the vapor-pressure curve used for NbC is lower than that of any other contender for this application. The curve used is, in fact, a rather optimistic guess at the vapor pressure of NbC. The impulse range for ZrC is from 1140 to 1350 seconds. Because of the relatively high vapor pressure of ZrC, a surface temperature of 10 000° R gives a lower maximum impulse than does 9000° R.

For a bubble-through system, reference 17 indicates 1340 seconds for ZrC and 1490 seconds for NbC, at a reactor pressure of 100 atmospheres. A specific impulse of 1450 seconds is predicted in reference 3 for ZrC at a reactor pressure of 100 atmospheres and a dilution ratio of 50 (which corresponds to the UC_2 mole fraction of 0.02 used herein). The results of reference 3 also indicate that there is little to be gained in

specific impulse by using more dilute fuels. If the dilution ratio is increased from 50 to 1000, the maximum specific impulse increases by about 100 seconds at most. The maximum specific impulse is virtually independent of reactor pressure in the range of 3 to 100 atmospheres (ref. 3). Thus, it is not likely that the specific impulse of a liquid-core reactor can exceed, to any appreciable extent, the values shown in figure 17.

For the 4-inch-diameter tube, the maximum impulse occurs at tube lengths between 10 and 20 feet for both NbC and ZrC diluents for wall temperatures between 9000° and $10\ 000^{\circ}$ R. The value of this optimum tube length is not, however, independent of either the hydrogen flow rate or the tube diameter. The heat-transfer results in figure 12 indicate that the tube length required to produce a given thermal effectiveness is directly proportional to both the tube diameter and the gas flow rate per unit area. These variations show that tube length can be reduced by decreasing either the tube diameter or the hydrogen flow rate per unit flow area. The choice between these two possibilities is determined by their effect on reactor size and thrust to weight ratio. The thrust to weight ratio can be written in terms of the parameters under discussion as

$$\frac{F}{W} = \frac{\bar{A}GI_{sp}}{(1 - \bar{A})\rho_r D \frac{L}{D}}$$

This equation leads to the conclusions that, because the outlet temperature is affected only by the ratio of G to L/D, the absolute values can be chosen on some other basis such as a criticality or mission requirement. A minimum tube diameter is needed to maximize the thrust to weight ratio. This minimum size would be determined by some other criterion such as seed density or rotational speed requirement.

Fuel loss rate. - In addition to specific impulse, the rate at which uranium is lost from the engine is significant. In the absence of any clear, quantitative limits placed by contamination, or economic and storage considerations, the fuel loss rate is presented relative to that of the hydrogen propellant. This fact permits an assessment of fuel loss on a basis that is essentially independent of mission.

Figure 18 shows the ratio of hydrogen flow rate to uranium flow rate as a function of tube length and liquid surface temperature for a 4-inch-diameter tube. Qualitatively, the curves exhibit a predictable characteristic, that longer tubes and higher fuel temperatures cause greater uranium loss rates.

The results shown in figure 18 are for a UC_2 mole fraction in the liquid fuel of 0.02. Obviously, the uranium loss rate is directly related to this quantity. This relation is illustrated in figure 19 where the hydrogen- to uranium-flow-rate ratio is shown as a function of UC_2 concentration for a fuel temperature of 9000° R. From figure 19, it is clear

that unlimited reduction of fuel loss can be achieved by decreasing the UC_2 concentration. Therefore, the concentration of UC_2 in the liquid fuel should be the minimum that is consistent with some other criterion such as criticality or engine life.

An increase in tube length affects both the fuel loss rate and the specific impulse of the engine. Thus, it is possible to compromise between these two parameters. This effect is shown in figure 20 for NbC and ZrC. The three solid curves are for the indicated surface temperatures of 9000°, 9500°, and $10\ 000^{\circ}$ R. The dashed curve is the locus of end points of the family of curves and represents the effluent from an infinitely long tube; that is, the propellant is at the liquid fuel temperature and is saturated with vapor of equilibrium composition. Thus, the dashed curve represents, in effect, the performance of a bubble-through system. A performance advantage of radiation heating over conduction is indicated wherever a solid line is above the dashed line.

These results show that radiation heating offers specific impulses that are only 70 seconds higher than the best available from a conduction heating process. Because of its lower vapor pressure, NbC allows higher specific impulses than does ZrC. With a NbC solvent, the highest surface temperature, $10\ 000^{\circ}$ R, gave the highest specific impulse, 1620 seconds. For ZrC, the lowest temperature considered, 9000° R, gave the highest specific impulse, 1370 seconds. Of course, further lowering of the ZrC surface temperature would not continue to give higher specific impulses without limit; it would reach some maximum and then decrease toward the bubble-through value. The general conclusion indicated is that radiation heating offers a specific impulse gain over a bubble-through system, but the advantage is a small one. It is therefore likely that the choice will be determined by some more compelling engine characteristic, such as the maximum hydrogen-flow-rate capability.

The numerical values of hydrogen- to uranium-weight-flow ratio shown in figure 20 are directly related to the reactor pressure of 100 atmospheres and the UC_2 concentration of 0.02 mole fraction. The ratio of hydrogen to uranium flow rate varies directly with reactor pressure (up to the point where the specific impulse of pure hydrogen is significantly reduced by increasing pressure) and inversely with uranium concentration in the fuel. The effect of varying uranium concentration is shown in figure 19. The effect of reactor pressure is illustrated in the following discussion.

At a pressure of 100 atmospheres, figure 20(a) shows that the hydrogen- to uranium-flow-rate ratio is about 20 for a specific impulse of 1400 seconds and a surface temperature of 9500° R. At a pressure of 200 atmospheres, the flow-rate ratio would be approximately 50; and at 400 atmospheres it would be about 100. Of course, the pressure cannot be increased without limit because the specific impulse of the pure hydrogen is reduced by increasing pressure. For example, at an outlet gas temperature of 8500° R, a specific impulse of 1400 seconds is not attainable for a pressure greater than 250 atmospheres. Thus, with the constraint of constant specific impulse, the uranium loss rate

cannot be adjusted to any desired value by arbitrarily increasing reactor pressure.

Sample Engine

Selection. - It is necessary to select a specific, dimensional configuration in order to present some of the engine characteristics in more detail. Although it would be desirable for this choice of a particular engine to be an optimum, or best one, the extent of this parametric study is insufficient for that purpose. Therefore, the sample engine that was chosen, while based on judicious selections, does not necessarily give the best performance attainable. The main value of a sample engine is that it allows the presentation of more detailed information about some engine characteristics not explicitly displayed in the parametric study. Such information includes radial fuel concentration and temperature profiles in the hydrogen at various axial positions down the length of the tube, temperature profiles in the liquid fuel and the surrounding solid structure, an estimate of engine weight based on a particular fuel-element geometry, and, finally, all the pertinent engine performance characteristics of the sample engine.

The sample engine was arbitrarily chosen to have a 3000-megawatt power level. Although the parametric study was conducted for a reactor pressure of 100 atmospheres, a value of 200 atmospheres was chosen for the sample case in order to reduce the ratio of nuclear fuel to hydrogen that is exhausted from the reactor. A fuel surface temperature of 9500° R, a tube diameter of 4 inches, a tube length to diameter ratio of 20, and a hydrogen mass velocity of 6.7 pounds per second per square foot were selected to give an engine specific impulse of 1400 seconds and reasonable values of engine length and thrust to weight ratio.

Radial profiles in gas. - The hydrogen propellant, seeded to have an opacity of 3, enters the tube at a temperature of 3500° R. As it flows through the tube, the bulk temperature of the gas approaches the surface temperature. Figure 21 shows the radial temperature profiles in the gas at various axial locations along the tube. The temperature jump at the tube surface is a result of neglecting conduction in the gas.

Figure 22 shows the corresponding concentrations in the sample engine. The vapor pressures used were those of a NbC/UC_2 fuel mixture with an 0.02 mole fraction of fuel in the mixture. At 9500° R, the equilibrium vapor pressure is 0.32 atmosphere. For a total pressure of 200 atmospheres, the mass fraction of heavy vapor in hydrogen at the liquid surface is 0.117. As indicated in figure 22, the bulk mass fraction of heavy vapor in the effluent from the tube is 0.03, or about 25 percent of the saturation value of 0.117. The concentration profiles were obtained by assuming similarity between concentration and velocity distributions; the profiles shown in figure 22 follow a 1/7 power variation with radial distance from the wall. This assumption should be reasonably accurate as

long as the primary flow is turbulent and the tube length to diameter ratio is greater than 15.

Temperature profiles in fuel and wall. - In addition to profiles in the flowing gas, the temperature distribution throughout the liquid fuel and supporting solid structure is of interest. The two important features to be considered are (1) the maximum internal temperature of the liquid fuel and (2) the temperature at the solid-liquid interface. Implicit in these two temperatures is the fraction of reactor power that is conducted radially outward from the fuel region. The simplest situation is one in which a uniformly fueled liquid is directly supported by a solid carbon tube. For the conditions of the sample engine, including the specification that only 25 percent of the generated heat is allowed to travel radially outward, the temperature profile within the fuel and the tube structure is shown in figure 23(a).

The upper curve was calculated by using the thermal conductivities of the liquid carbide and the solid carbon (300 and 26 Btu/(hr)(ft^2)($^\circ$F/in.), respectively). If it is assumed that the profile shown is stable, this curve clearly indicates two serious problems that are a direct result of transferring the internally generated heat to the propellant at one surface rather than throughout the fuel as is the case for the bubble-through system. The first undesirable situation is that internal fuel-region temperatures are excessively high, perhaps near or equal to the boiling point. The second problem is that the interface temperature must be maintained only 600° less than the maximum liquid temperature in order to drive 75 percent of the internally generated heat radially inward to the fuel surface where it is then radiated to the flowing propellant. For the sample engine, the maximum internal fuel temperature is 16 100° R and the fuel-carbon interface temperature is 15 500° R, if direct contact between the solid and the liquid is assumed.

The liquid-fuel region from the inner surface to the point of maximum temperature is potentially unstable because of the density gradient associated with the temperature profile. Any resultant free convection would tend to set up one or more "cells," and the net effect would be to decrease the resistance to heat flow toward the inner surface. Any turbulence propagated into the liquid from the flowing gas would have the same effect. The influence of both of these factors can be expressed in terms of an "effective" thermal conductivity that is higher than the actual value. The lower curve in figure 23(a) shows the extreme limit of this effect. It can be seen that even if thermal stirring of some sort does bring down the maximum temperature in the liquid fuel, the interface temperature is still beyond the melting point of any solid material.

It is possible, at least in principle, to reduce the liquid-solid interface temperature by introducing an unfueled liquid region between the fuel and the carbon. Figure 23(b) shows the temperature profiles for such a situation. The curves correspond to these in figure 23(a). The upper curve, computed by using true thermal conductivities, shows that the addition of a 0.2-inch-thick layer of unfueled liquid carbide decreases the inter-

face temperature only from 15 000° to 12 900° R. If, in addition to an unfueled liquid region, thermal stirring is present in the unstable portion of the fueled liquid, the interface temperature is 6300° R. Since this temperature is near a maximum acceptable solid surface temperature (carbon sublimes at 7200° R) and was calculated by simultaneously invoking turbulence in the fueled region and no migration of fuel into the unfueled region, it does not appear to be a reasonable possibility. Further, if no thermal stirring does occur, a thick, and therefore heavy, region of unfueled liquid carbide is necessary to reduce the interface temperature. The net conclusion from figure 23 seems to be that floating the liquid fuel on an insulating film or layer of unfueled liquid is not a promising technique to protect the solid wall from overheating.

It is also possible to reduce the difference between the interface temperature and the maximum fuel temperature by reducing the fuel region thickness. Of course, this cannot be done without bound because of criticality and mass-transfer limitations, but an estimate of the effect is informative. This temperature difference is shown in figure 24 as a function of fuel region thickness. The sample engine condition is shown; the fuel region thickness is 0.375 inch, and the maximum fuel temperature is 600° R higher than that of the carbon surface. The general conclusion from figure 24 is that the difference between the maximum internal fuel temperature and the interface temperature cannot be dramatically altered by changing the fuel region thickness; the maximum possible effect is of the order of a few hundred degrees.

Other fuel support considerations. - Since it may be difficult to prevent heat flow into the solid structure at temperatures below the sublimation temperature of carbon, it is of interest to consider how much sublimation is tolerable. For the sample engine, the reactor power level is 3000 megawatts. If 25 percent of this power is conducted radially outward, the heat flux into the carbon surface is 7.1 Btu per second per square inch. Using 15 000 Btu per pound as the heat of sublimation, the carbon tube wall would erode at a rate of 1/2 inch per minute. For a reasonable fuel element configuration, the carbon thickness would probably be from $\frac{1}{2}$ to 1 inch. Thus, it is not possible to accommodate any appreciable fraction of reactor power by sublimation because of direct contact of the liquid fuel with the carbon structure, unless the vapor film formed reduces the heat flux to the wall.

To put the situation in proper perspective, the heat- and mass-transfer calculations show that, in principle, there is some advantage in transferring the fission energy from the liquid fuel to the propellant by radiation rather than by conduction. However, it is necessary to operate at liquid surface temperatures from 9000° to 10 000° R in order to achieve this advantage. This requirement leads to a temperature at the liquid-solid interface that is above the reported triple-point temperature of carbon if there is direct liquid-solid contact. Such a condition does not appear to be tenable if no vapor film forms because (1) if the reactor pressure is below the triple-point pressure of 110 atmos-

pheres, the solid carbon would sublime too fast; or (2) if the pressure is above 110 atmospheres, the carbon would melt, permitting migration of fuel radially outward followed by further melting of the structural carbon.

There are a limited number of ways to resolve the problem. The following list presents some possible solutions, although not in any particular order.

(1) The liquid-solid interface may be eliminated by employing some force other than physical support to hold the liquid fuel in the engine, for example, suspending liquid drops in a flowing gas stream by some body force.

(2) The interface temperature may be reduced to below 7200° R by flowing some of the propellant radially inward through the solid and liquid regions. The performance of such a hybrid flow system would have to be compared with that of the pure bubble-through configuration. Preliminary estimates indicate that at least 25 percent of the total propellant flow would have to be bubbled through the liquid in order to keep the interface temperature below 7200° R. Such a result is dependent on the effective thermal conductivity of the liquid fuel, which can be strongly affected by turbulence and free convection.

(3) The interface temperature may be reduced by operating below 110 atmospheres and supporting the liquid on an insulating vapor film of carbon, or some other material, that would form during an initial transient. This situation is similar to a drop of water that is insulated from a hot surface by the formation of a layer of steam.

(4) The triple-point temperature of carbon may actually be higher than the reported 7200° R. Although remote, this possibility cannot be eliminated because of an apparent anomaly between vapor-pressure measurements and liquid-solid equilibrium data (ref. 11).

Engine weight. - In addition to internal temperature distributions, engine weight is an important characteristic of interest. Figure 25 illustrates a particular fuel element configuration chosen for the purpose of making a weight estimate. The metallic carbide contributes over 40 percent of the reactor core weight. For the 3000-megawatt sample engine with a 4-inch-inside-diameter fuel element, the reactor core weight is 26 000 pounds. The engine is composed of 100 fuel-element tubes through which hydrogen flows at 59 pounds per second. At a specific impulse of 1400 seconds, the engine thrust is 83 000 pounds; the thrust to core-weight ratio is thus 3. 2. All the parameters of interest for this sample engine are summarized in table II.

The actual thrust to core-weight ratio can be adjusted to a desired level by changing the tube diameter. Of course, there are practical limitations on such a variation that would result from mechanical design problems and nuclear scaling characteristics. The major sample engine parameters are shown in table III for tube diameters of 1, 2, and 4 inches to illustrate the effect of changing tube diameter. Engine thrust to core weight increases, because of decreasing engine size and weight, as tube diameter is reduced.

TABLE II. - BASIC SAMPLE ENGINE VARIABLES

Geometry	
Engine diameter, ft	6.7
Engine length, ft	6.7
Number of tubes	100
Fuel element	
Niobium carbide and 0.02 mole fraction uranium carbide	
Rotating speed, rpm	2400
Tube diameter, in.	4
Core length, ft	6.7
Flow rates, lb/sec	
Hydrogen	59
Uranium	1.2
Other	0.4
Weight, lb	
Reactor core	26 000
Uranium carbide (U, 230 kg)	556
Niobium carbide	11 100
Carbon	8500
Water	3400
Aluminum	2200
Operating conditions	
Temperature, ^{o}R	
Hydrogen inlet, $T_{H_2,1}$	3500
Hydrogen outlet, $T_{H_2,2}$	8450
Liquid surface, T_s	9500
Reactor pressure, atm	200
Performance	
Reactor power, MW	3000
Thrust, lb	84 000
Specific impulse, sec	1400

TABLE III. - EFFECT OF TUBE DIAMETER ON MAJOR ENGINE PARAMETERS

Engine parameters	Tube diameter, in.		
	1	2	4
Number of tubes	640	250	100
Core diameter, ft	4.2	5.3	6.7
Core length, ft	4.2	5.3	6.7
Uranium 235 critical mass, kg	58	115	230
Core weight, lb	6500	13 000	26 000
Hydrogen flow rate, lb/sec	59	59	59
Radiant heat flux, kW/in.^{2}	22	22	22
Reactor power level, MW	3000	3000	3000
Specific impulse, sec	1400	1400	1400
Engine thrust, lb	84 000	84 000	84 000
Thrust to core weight ratio	13	6.5	3.2

This trend would continue until the specific impulse was decreased because of an increase in the required mass fraction of seed material. The actual compromise to be considered in an engine selection would balance decreased engine weight against increased mechanical and/or heat-transfer complexities associated with an increased number of tubes.

Table III also can be used to illustrate that the thrust to weight ratio is independent of thrust level. Consider the column for a 1-inch-diameter tube. The engine described consists of 640 tubes that are 4.2 feet long and has a thrust of 84 000 pounds. As long as the tube diameter is 1 inch and the length is 4.2 feet, the thrust to weight ratio remains at 13, independent of the number of tubes. However, the thrust level is proportional to the number of tubes. Thus, 64 tubes would give a thrust of 8400 pounds; 640 tubes give 84 000 pounds of thrust, as shown in table III; and 6400 tubes would give 840 000 pounds of thrust.

CONCLUDING REMARKS

A parametric performance study was conducted for a liquid-core nuclear rocket engine in which the hydrogen is heated by absorbing thermal radiation from the surface of a liquid-metal carbide solvent that contains uranium carbide. Calculations were made (1) to describe some of the important heat- and mass-transfer characteristics of such an engine, and (2) to determine if such a system offers any significant performance advantage over a bubble-through system in which the propellant is heated by conduction as it passes radially inward through the solid and liquid regions of a fuel element. In both configurations, the hot liquid-carbide fuel is held in place on the inner surface of a rotating tube.

In all the parameter calculations, the hydrogen propellant was assumed to enter the tubular flow passage at a temperature of 3500° R. The primary variables considered, and the values used, were as follows:

(1) Mole fraction of uranium carbide in solvent . . . . . 0.002, 0.01, and 0.05
(2) Fuel surface temperature, ^{o}R . . . . . 9000, 9500, and 10 000
(3) Hydrogen mass velocity, lb/(sec)(ft^2) . . . . . 1, 3, and 10
(4) Tube diameter, in. . . . . 1 to 8
(5) Tube length, ft . . . . . 5, 10, and 15
(6) Fuel solvent . . . . . ZrC, NbC

On the basis of the parametric calculations, a sample engine was chosen to permit a more detailed and specific description of some engine characteristics such as internal temperature distributions. From these calculations, a general picture of such a liquid-fueled engine has emerged. However, it is not reasonable to describe the engine by assigning one numerical value to each of the major parameters, such as specific impulse, tube diameter, and thrust to core-weight ratio, because one parameter can be increased, within limits, at the expense of another. For example, thrust to core-weight ratio can be increased by decreasing the tube diameter, but this, in turn, causes an increase in the total number of tubes in an engine of fixed, overall length to diameter ratio. Similarly, the ratio of hydrogen to uranium in the exhaust mixture can be increased by increasing the reactor pressure, but this eventually decreases the specific impulse unless higher surface temperatures are used.

Because of this interdependence, engine characteristics are given as a range of values. For most of the parameters, the lower limit simply defines the bounds of acceptable performance; for example, a specific impulse less than 1300 seconds is readily obtainable but too low to be of much interest. The upper limit is either one that cannot be exceeded (e. g. , specific impulse) or that would not be exceeded because of an adverse compromise with some other parameter (e. g. , thrust to core weight ratio can easily exceed 13, but the accompanying decrease in hydrogen- to uranium-flow-rate ratio would probably override the advantage). Finally, it should be pointed out that all combinations of parameters are not available; that is, the best value of one parameter may be available only at the expense of another. Thus, the maximum values of specific impulse, thrust to weight ratio, and hydrogen- to uranium-flow-rate ratio cannot be obtained together.

CONCLUSIONS

The parametric calculations and the sample engine provide quantitative estimates of the major engine characteristics of a liquid-core nuclear rocket engine that employs radiant heating of the hydrogen propellant. These results are

1. Specific impulse ranges from about 1300 to 1600 seconds. The upper limit is the

maximum attainable and is only about 70 seconds higher than that produced by conduction heating in a bubble-through system.

2. To obtain the range of specific impulse of 1300 to 1600 seconds, the liquid-fuel surface temperature must be between 9000° and $10\,000^{\circ}$ R. Since this temperature exceeds the highest known melting point (the triple-point temperature of carbon is reported to be 7200° R), a major problem exists in trying to support the fuel.

3. The thrust to reactor-core-weight ratio ranges from 3 to 13 and is independent of the absolute thrust level. An important influence on this parameter is the tube diameter. Thrust to weight ratio can be increased by using smaller tube diameters; however, this compromise is made at the expense of an increase in the total number of tubes.

4. The hydrogen- to uranium-flow-rate ratio ranges from 20 to 100. Values above 20 are achieved by increasing the reactor pressure. Eventually, however, this increase in pressure either decreases the specific impulse or requires a higher surface temperature, making it undesirable to increase the hydrogen to uranium ratio above 100.

5. To be consistent with the foregoing ranges, the tube diameter should be between 1 and 4 inches and the reactor pressure should be in the range of 100 to 1000 atmospheres.

Lewis Research Center,
National Aeronautics and Space Administration,
Cleveland, Ohio, February 23, 1967,
122-28-02-18-22.

APPENDIX - SYMBOLS

$\overline{A}$	free-flow factor of reactor
B	mass-transfer parameter (see eq. (10))
C	mass fraction
c_p	specific heat, Btu/(lb)(^oR)
D	tube diameter, in.
F	thrust, lb
f	friction factor
G	mass velocity, lb/(sec)(ft^2)
g	gravitational constant, ft/sec^2
H	enthalpy, Btu/lb
h_d	mass-transfer coefficient, ft^2/sec
h_{do}	mass-transfer coefficient at negligible mass-transfer rates, ft^2/sec
I_{sp}	specific impulse, sec
I^*_{sp}	specific impulse of pure hydrogen, sec
J	mechanical work equivalent of heat, (ft-lb)/Btu
j	j-factor (see eq. (11))
K	gray gas absorption coefficient, ft^{-1}
k	thermal conductivity, (Btu)(in.)/(hr)(ft^2)(^oR)
L	tube length, ft
Δl	incremental thickness, in.
M	molecular weight
$\overline{M}$	propellant average molecular weight
$\overline{M}_v$	heavy vapor average molecular weight
N	molar flux at liquid surface, moles/(ft^2)(sec)
$\hat{n}$	unit direction vector
P	equilibrium vapor pressure, atm
P_r	reactor pressure, atm
P^o	vapor pressure, atm
p	partial pressure, atm
Q_r	total reactor power, MW
Q'	reactor power to raise propellant temperature to T_2
q''	heat flux, Btu/(ft^2)(sec)
q'''	volumetric heat-generation rate, Btu/(ft^3)(sec)
R	flow passage radius, in.
r	radial coordinate, in.
$\hat{r}$	unit direction vector
T	temperature, ^oR
V	volume, ft^3
v	axial velocity
W	weight, lb
$\dot{w}$	mass flow rate, lb/sec
X	mole fraction in liquid
Y	mole fraction in vapor
z	axial coordinate, ft

α	correction factor for mixture specific impulse
ϵ	emissivity
θ	ratio of actual mass-transfer coefficient to mass-transfer coefficient at negligible mass-transfer rates, h_d/h_{do}
μ	viscosity
ρ	density
σ	Stephan-Boltzmann constant, $Btu/(ft^2)(sec)(^oR^4)$
τ	opacity, KD
ψ	reactor power fraction in solid structure

Subscripts:

b	bulk
C	carbon
e	emission point
f	field point
H_2	hydrogen
i	i^{th} component
int	fuel-structure interface
j	remaining components
ℓ	liquid fuel
NbC	niobium carbide
p	propellant
r	reactor
s	liquid surface
UC_2	uranium carbide
U	uranium
v	vapor
w	wall
XC	NbC or ZrC
ZrC	zirconium carbide
1	reactor inlet
2	reactor outlet

REFERENCES

1. Cooper, Ralph S., ed.: Proceedings of an Advanced Nuclear Propulsion Symposium. Rep. No. LA-3229-MS, Los Alamos Scientific Lab., Jan. 1965.

2. Barrett, W. Louis, Jr.: Liquid-Core Nuclear Rocket. Paper No. 64-541, AIAA, May 1964.

3. Nelson, Seymour T.; Grey, Jerry; and Williams, Peter M.: Conceptual Study of a Liquid-Core Nuclear Rocket. J. Spacecraft Rockets, vol. 2, no. 3, May-June 1965, pp. 384-391.

4. Wood, L.; and Jensen, C.: Third Report on Nuclear Rocket Propulsion. Department of Chemistry, University of California, Los Angles, 1964.

5. Honig, R. E.: Vapor Pressure Data for the Solid and Liquid Elements. RCA Rev., vol. 23, no. 4, Dec. 1962, pp. 567-586.

6. Fries, R. J.: Vaporization Behavior of Niobium Carbide. J. Chem. Phys., vol. 37, no. 2, July 15, 1962, pp. 320-327.

7. Speidel, E. O.: Fabrication of Ceramic Fuels other than Uranium-Oxide. Reactor Core Materials, vol. 4, no. 4, Nov. 1961, pp. 13-16.

8. Anon.: Handbook of Chemistry and Physics. 37th ed. Chemical Rubber Publ. Co., 1955-1956, pp. 2013-2018.

9. Coffman, J. A.; Culson, K. L.; and Kibler, G. M.: Carbonization of Plastics and Materials Research Program. Fourth Quarterly Progr. Rep., Flight Propulsion Lab., General Electric Co., Cincinnati, Dec. 1960. Contract No. AF 33(616)-6841.

10. Kaufman, L.; and Peters, E. T.: Analyses of Vaporization in Liquid Uranium Bearing Systems at Very High Temperatures. Manlabs, Inc. (NASA CR-353), Dec. 1965.

11. Kaufman, L.; and Peters, E. T.: Analysis of Vaporization of Liquid Uranium, Metal, and Carbon Systems at 9000° and $10,000^{\circ}$ R. Manlabs, Inc. (NASA CR-591), Sept. 1966.

12. Einstein, Thomas H.: Radiant Heat Transfer to Absorbing Gases Enclosed in a Circular Pipe with Conduction, Gas Flow, and Internal Heat Generation. NASA TR R-156, 1963.

13. Kascak, Albert F.: Coaxial Flow Radiation Heat Transfer Analysis. Proceedings of an Advanced Nuclear Propulsion Symposium. Ralph S. Cooper, ed. Rep. No. LA-3229-MS, Los Alamos Scientific Lab., Jan. 1965, pp. 208-221.

14. Bird, R. Byron; Stewart, Warren E.; and Lightfoot, Edwin N.: Transport Phenomena. John Wiley & Sons, Inc., 1960, p. 658.

15. King, Charles R.: Compilation of Thermodynamic Properties, Transport Properties, and Theoretical Rocket Performance of Gaseous Hydrogen. NASA TN D-275, 1960.

16. Marteney, P. J.; Krascella, N. L.; and Burwell, W. G.: Experimental Refractive Indices and Theoretical Small-Particle Spectral Properties of Selected Metals. Rep. No. D-910092-6 (NASA CR-68865), United Aircraft Corp., Sept. 1965.

17. Kane, J. S.; and Wells, W. M., Jr.: Fundamental Materials Limitations in Heat-Exchanger Nuclear Rockets. Paper No. 65-530, AIAA, July 1965.

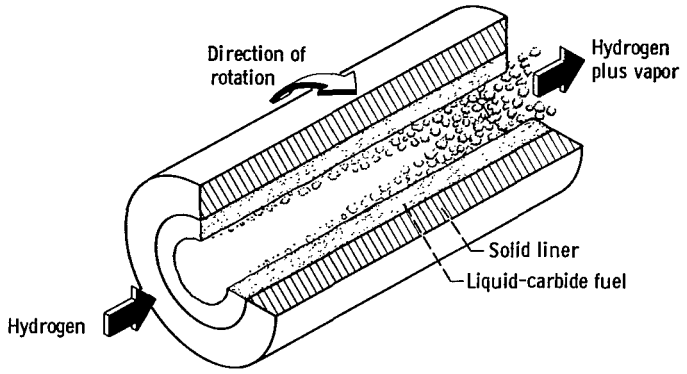

(a) Schematic diagram.

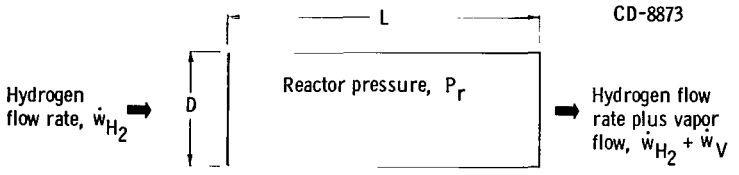

(b) Calculational model. Known gas properties: specific heat, viscosity, and opacity.

Figure 1. - Reactor flow passage.

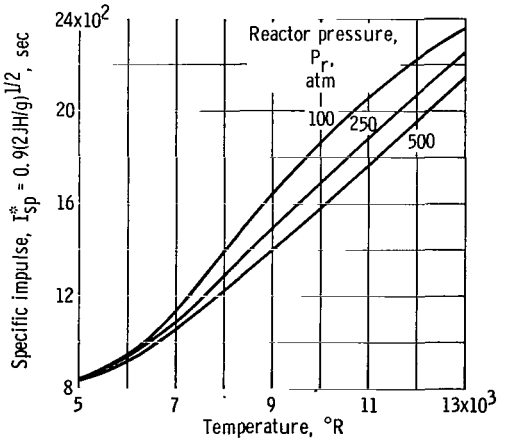

Figure 2. - Equilibrium specific impulse of hydrogen.

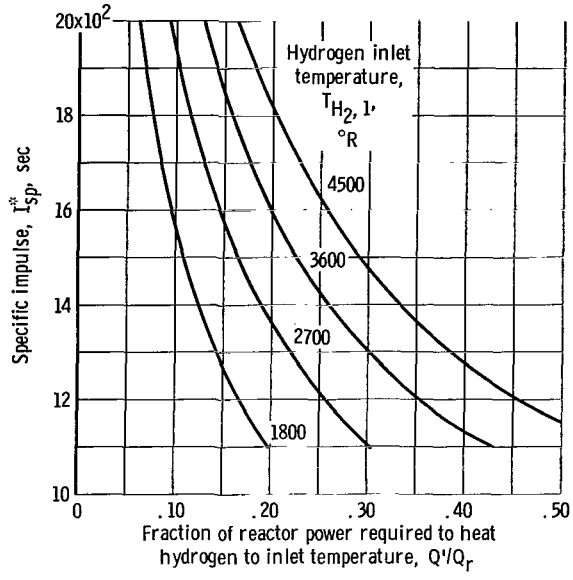

Figure 3. - Heat-balance limitation on engine specific impulse for reactor pressure of 100 atmospheres and pure hydrogen propellant.

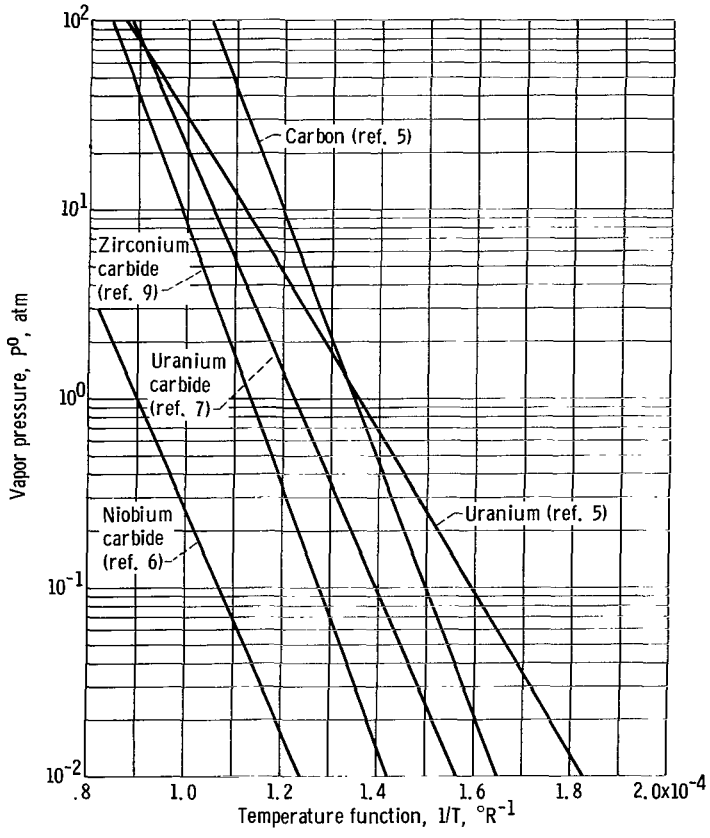

Figure 4. - Comparison of vapor pressures.

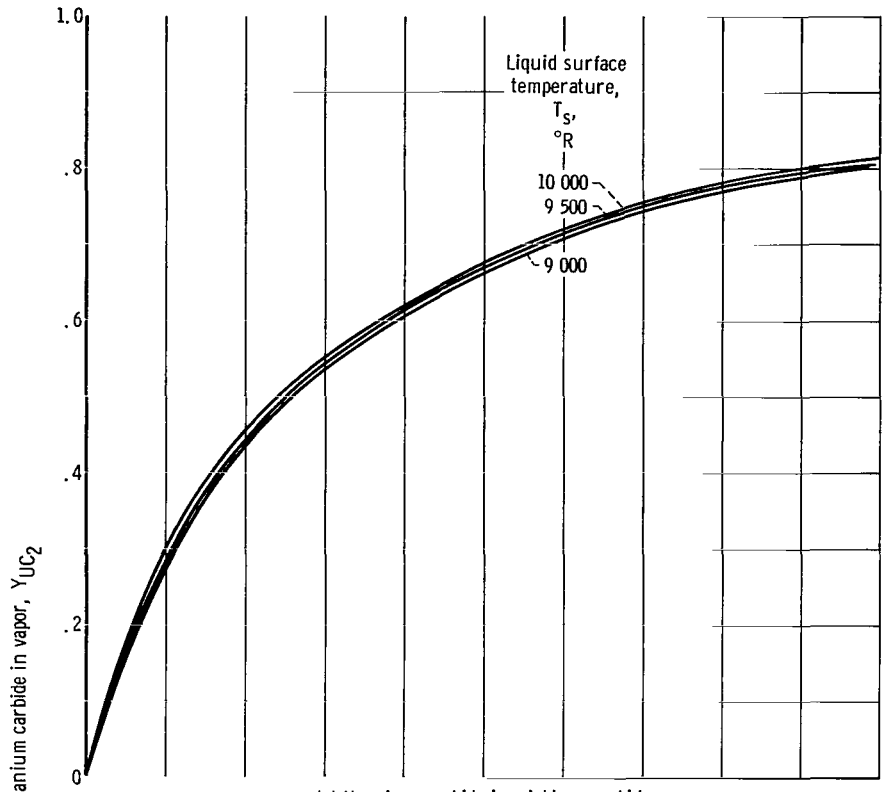

(a) Uranium carbide in niobium carbide.

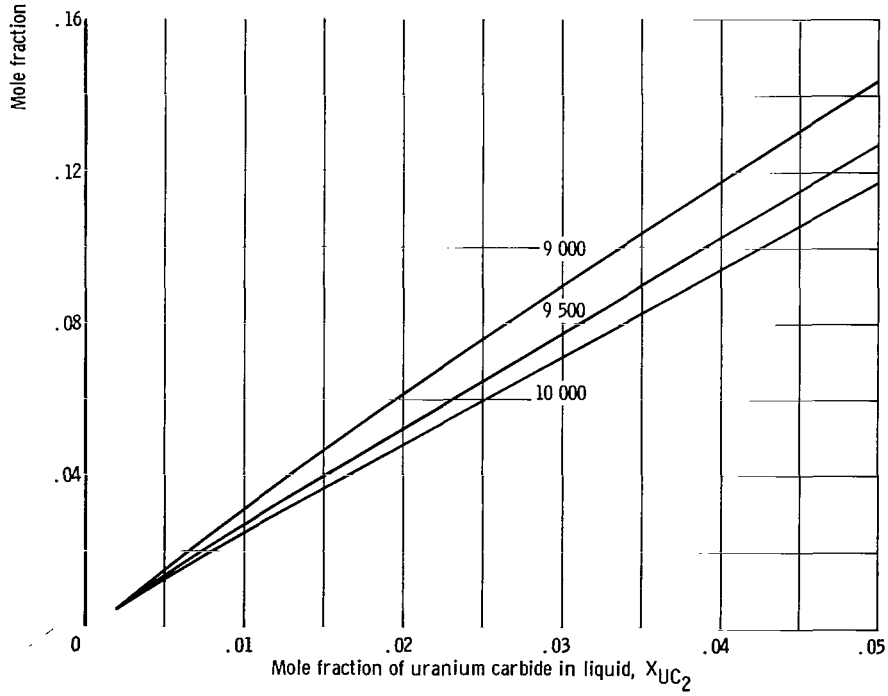

(b) Uranium carbide in zirconium carbide.

Figure 5. - Equilibrium vapor composition over liquid-fuel mixtures.

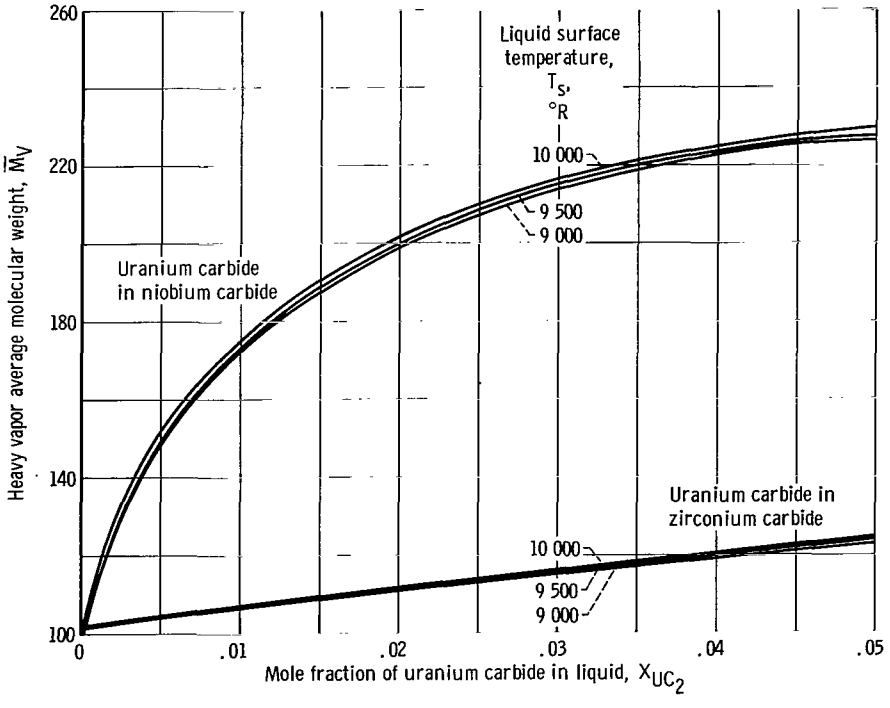

Figure 6. - Average molecular weight of vapor above liquid-fuel (UC_2/XC) system.

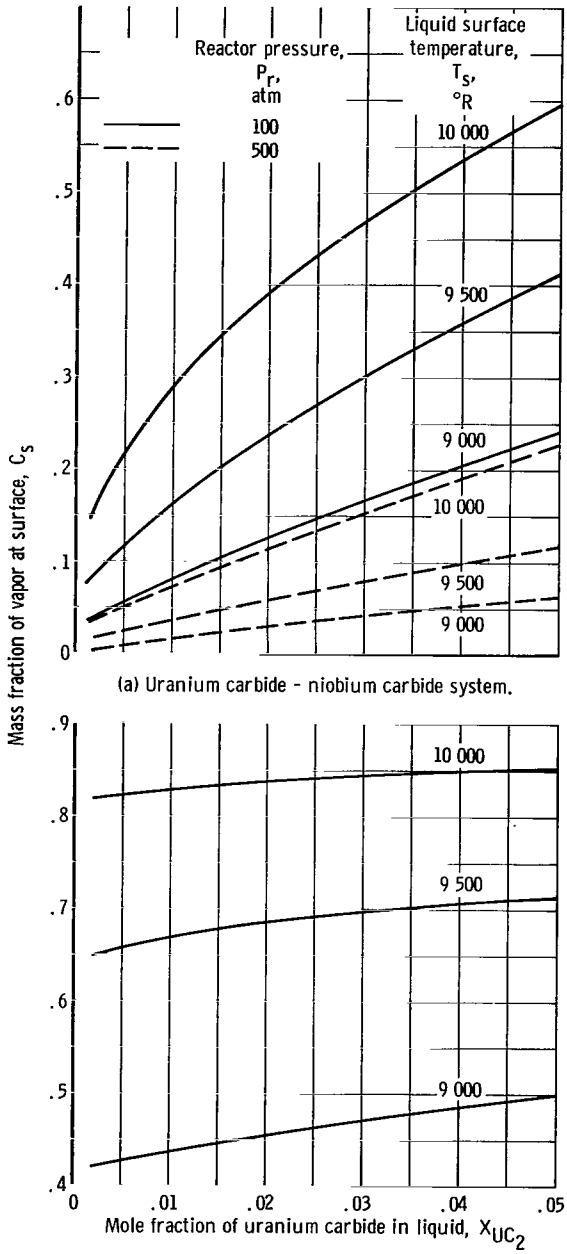

(a) Uranium carbide - niobium carbide system.

(b) Uranium carbide - zirconium carbide system.

Figure 7. - Mass fraction of heavy vapor in hydrogen at liquid-vapor interface.

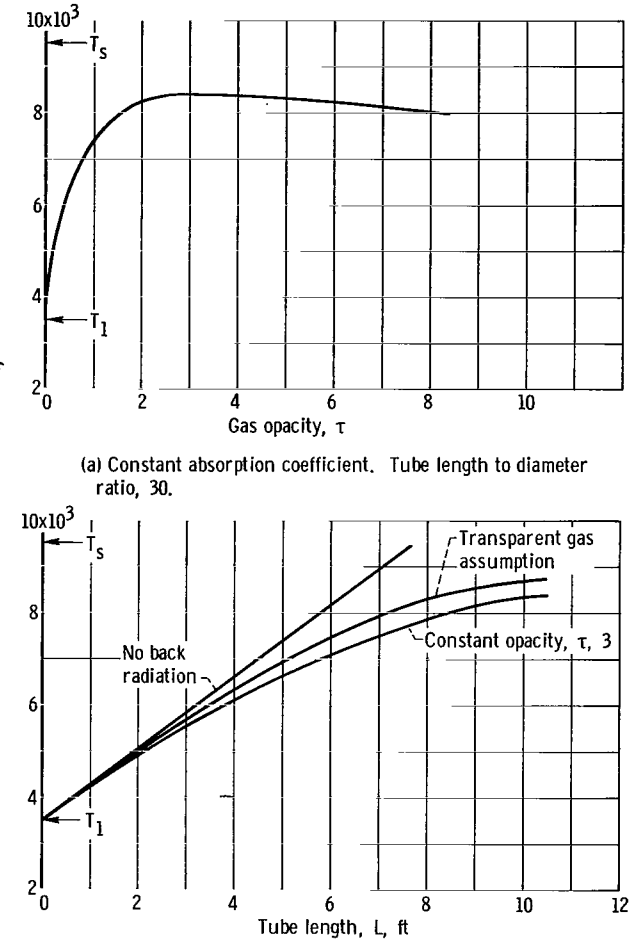

(a) Constant absorption coefficient. Tube length to diameter ratio, 30.

(b) Comparison of opacity assumptions. Tube diameter, 4 inches.

Figure 8. - Effect of gas opacity on hydrogen bulk outlet temperature. Liquid surface temperature, 9500° R; reactor inlet temperature, 3500° R; hydrogen mass velocity, 10 pounds per second per square foot; specific heat, 6 Btu per pound per °R.

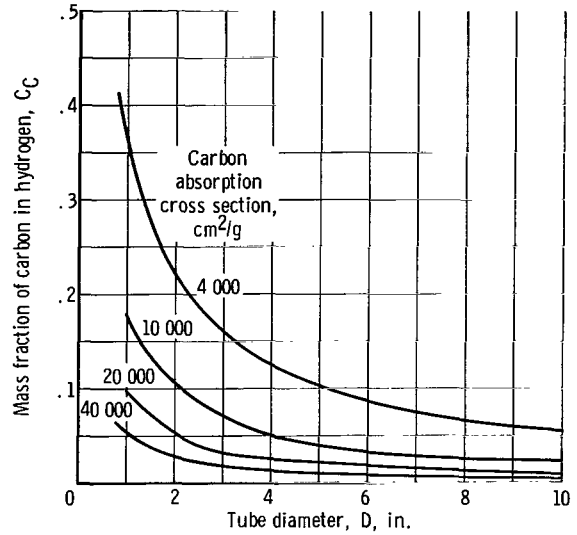

Figure 9. - Mass fraction of carbon in hydrogen for maximum heat transfer. Opacity, 3; reactor pressure, 100 atmospheres; hydrogen temperature, 8500° R.

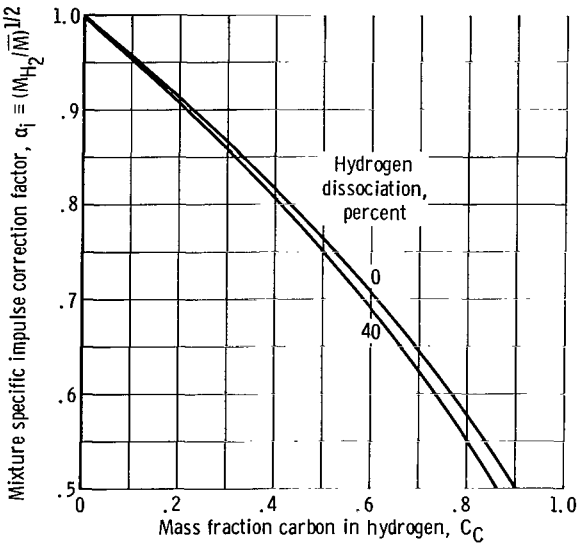

Figure 10. - Effect of carbon addition to hydrogen on mixture specific impulse.

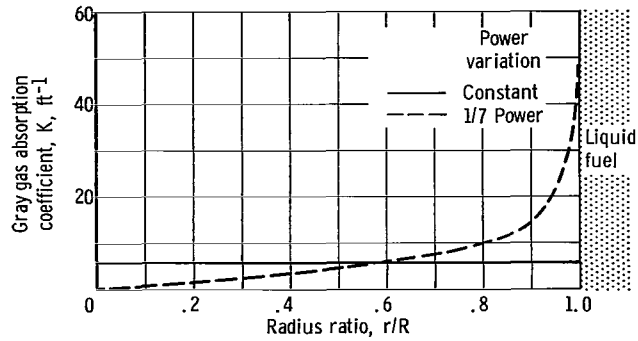

(a) Radial variation of absorption coefficient.

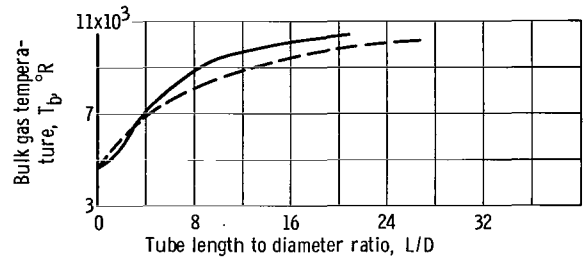

(b) Bulk gas temperature. Liquid surface temperature, 9500° R; reactor inlet temperature, 3500° R.

Figure 11. - Influence of radial variation of absorption coefficient on heat transfer to gas. Opacity, 3; hydrogen mass velocity, 3 pounds per second per square foot; specific heat, 6 Btu per pound per °R.

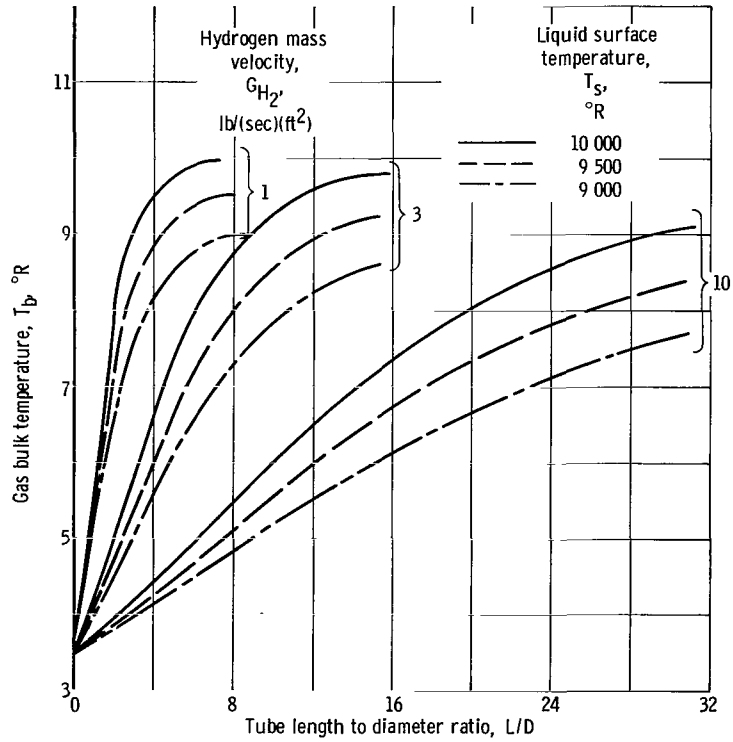

Figure 12. - Basic heat transfer. Gas opacity, 3; specific heat, 6 Btu per pound per °R.

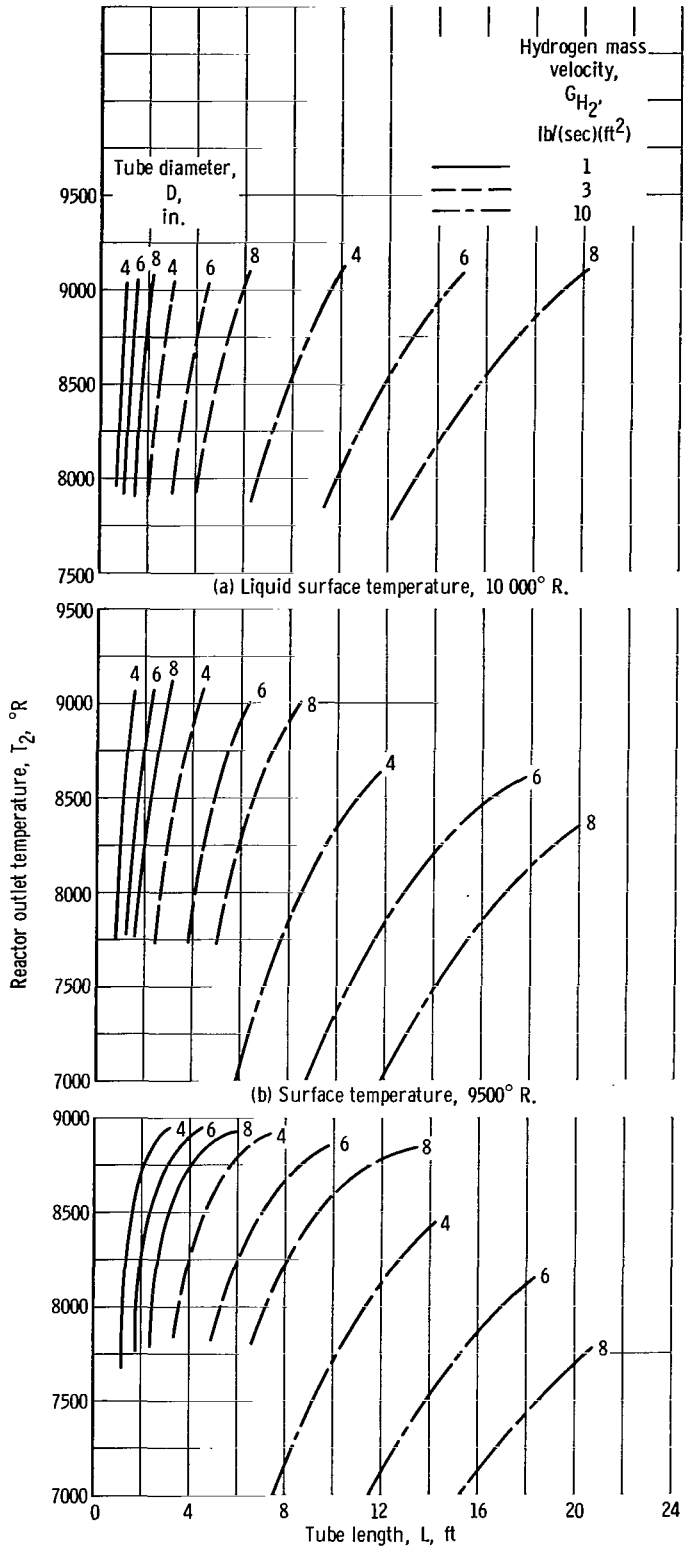

Figure 13. - Reactor outlet temperature as function of tube dimensions for hydrogen inlet temperature of 3500° R.

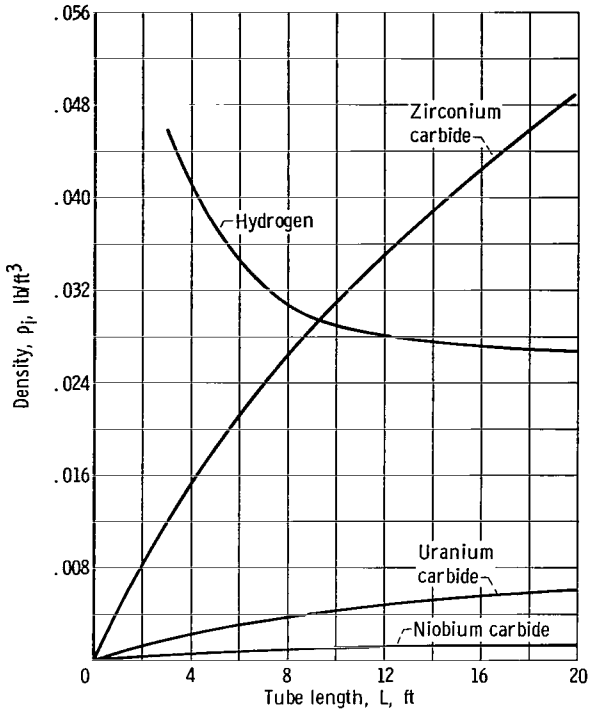

Figure 14. - Bulk composition as function of tube length. Reactor pressure, 100 atmospheres; surface temperature, 10 000° R; hydrogen mass velocity, 10 pounds per second per square foot; tube diameter, 4 inches; mole fraction of uranium carbide in liquid fuel, 0.02.

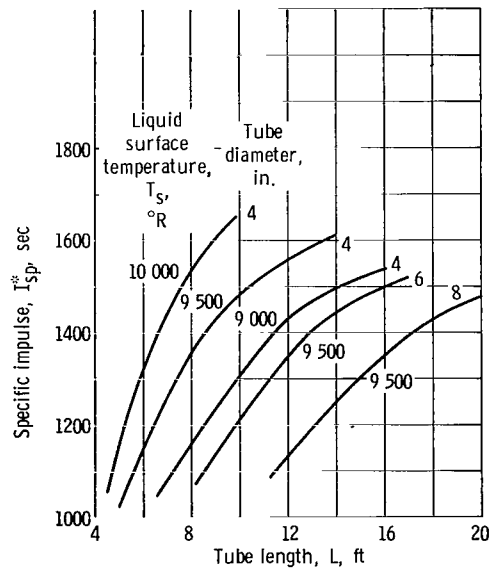

Figure 15. - Pure hydrogen specific impulse for various tube dimensions and surface temperatures. Reactor pressure, 100 atmospheres; hydrogen mass velocity, 10 pounds per second per square foot.

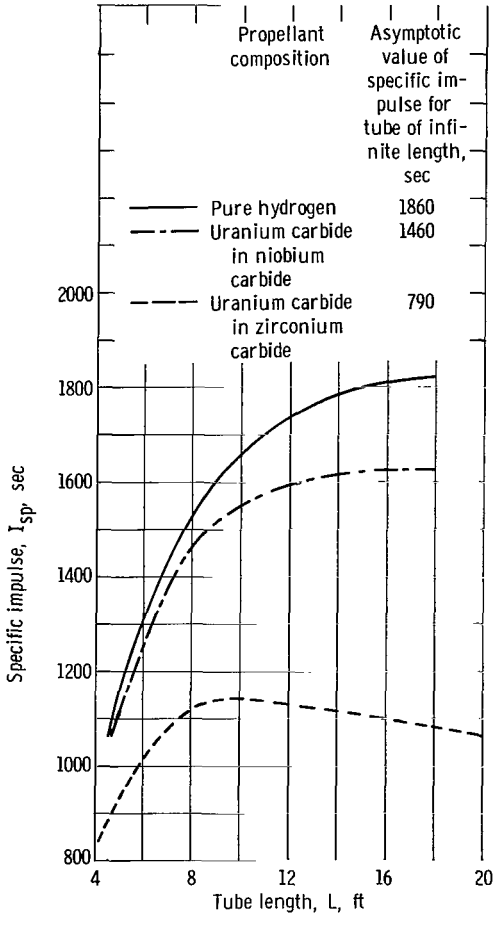

Figure 16. - Effect of heavy vapor on specific impulse. Reactor pressure, 100 atmospheres; surface velocity, 10 pounds per second per square foot; tube diameter, 4 inches; mole fraction of uranium carbide in liquid fuel, 0.02.

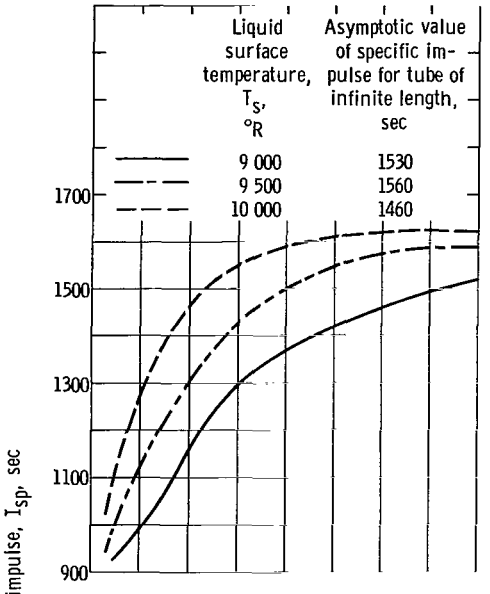

(a) Uranium carbide - niobium carbide system.

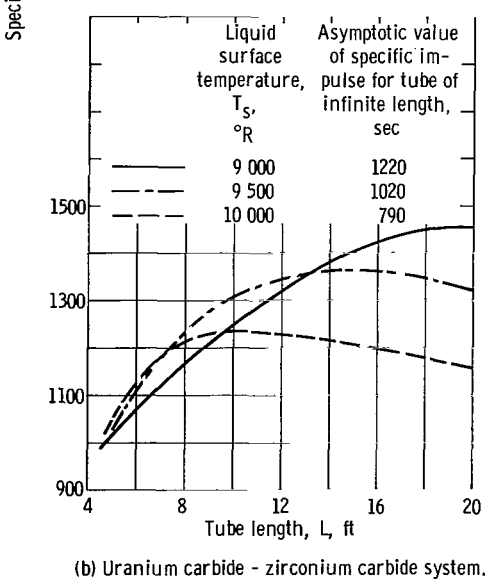

(b) Uranium carbide - zirconium carbide system.

Figure 17. - Effect of tube length and surface temperature on specific impulse. Reactor pressure, 100 atmospheres; hydrogen mass velocity, 10 pounds per second per square foot; tube diameter, 4 inches; mole fraction of uranium carbide in liquid fuel, 0.02.

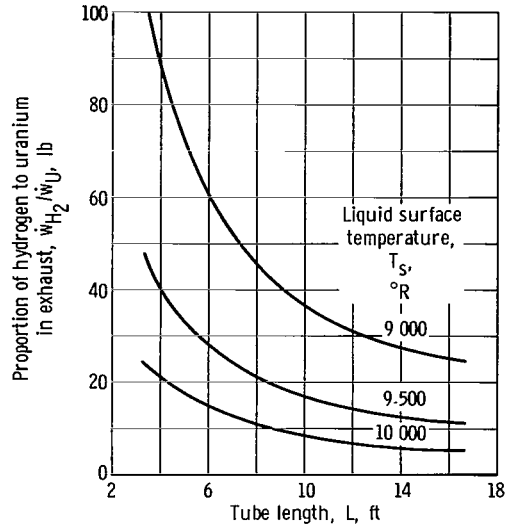

Figure 18. - Uranium loss. Reactor pressure, 100 atmospheres; hydrogen mass velocity, 10 pounds per second per square foot; tube diameter, 4 inches; mole fraction of uranium carbide in liquid fuel, 0.02.

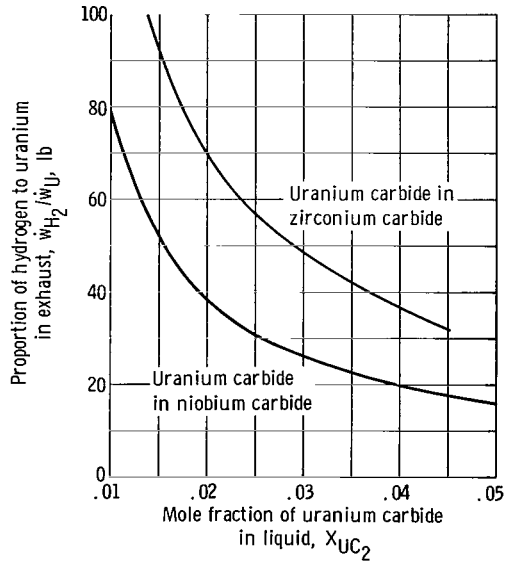

Figure 19. - Effect of concentration of uranium carbide in carbide system on uranium loss. Reactor pressure, 100 atmospheres; surface temperature, 9000° R; hydrogen mass velocity, 10 pounds per second per square foot; tube diameter, 4 inches; tube length, 10 feet.

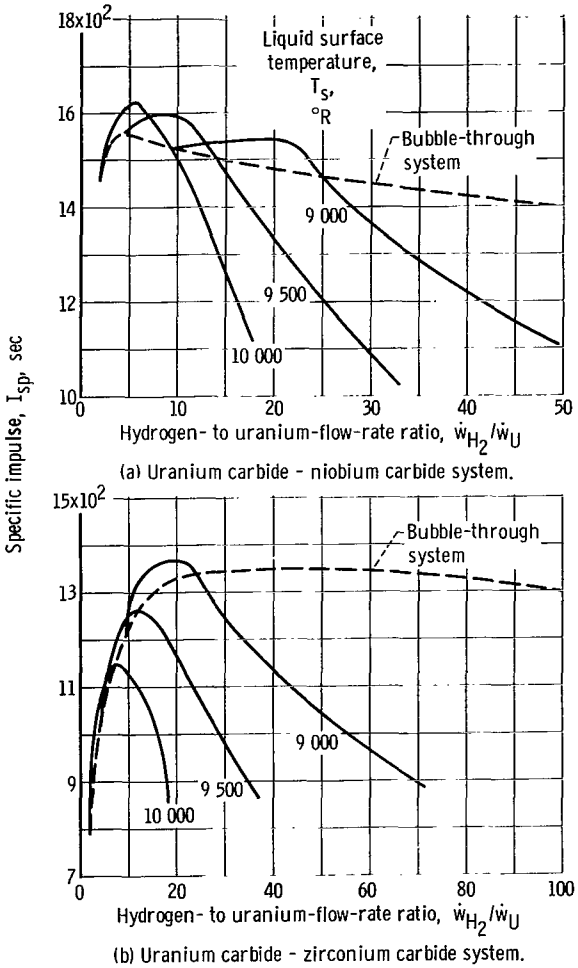

(a) Uranium carbide - niobium carbide system.

(b) Uranium carbide - zirconium carbide system.

Figure 20. - Compromise between uranium loss and specific impulse. Reactor pressure, 100 atmospheres; hydrogen mass velocity, 10 pounds per second per square foot; mole fraction of uranium carbide in liquid fuel, 0.02; tube diameter, 4 inches.

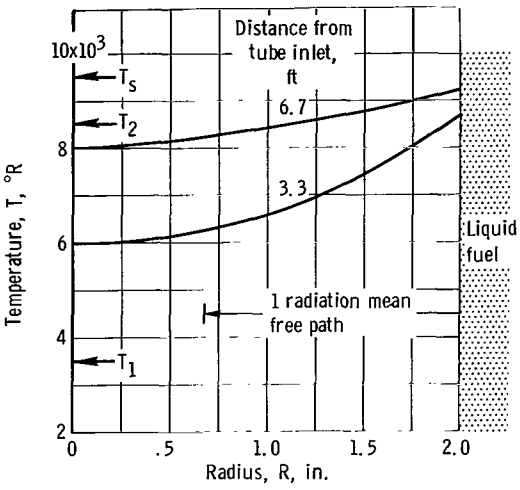

Figure 21. - Hydrogen temperature distribution for sample case. Hydrogen flow rate, 0.59 pounds per second; power delivered to hydrogen, 22.5 megawatts; reactor inlet temperature, 3500° R; reactor outlet temperature, 8450° R; liquid surface temperature, 9500° R.

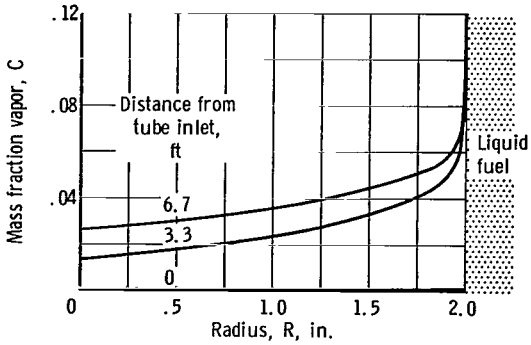

Figure 22. - Concentrations of heavy vapor for sample case. Reactor pressure, 200 atmospheres; partial pressure of vapor, 0.32 atmospheres; mass fraction at liquid surface, 0.117; bulk mass fraction, 0.03.

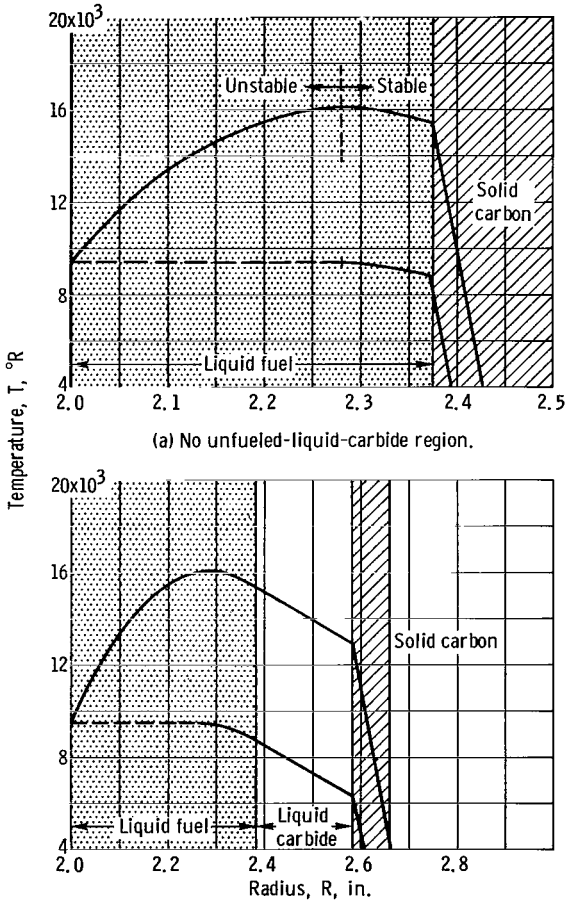

Figure 23. - Temperature distribution in liquid and wall, sample case. Fraction of reactor power required to heat hydrogen to inlet temperature, 0.25. Dashed portion of curve indicates thermal stirring ($R = \infty$).

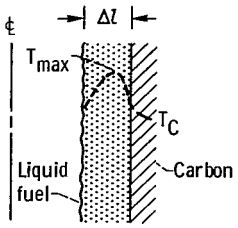

(a) Typical temperature distribution.

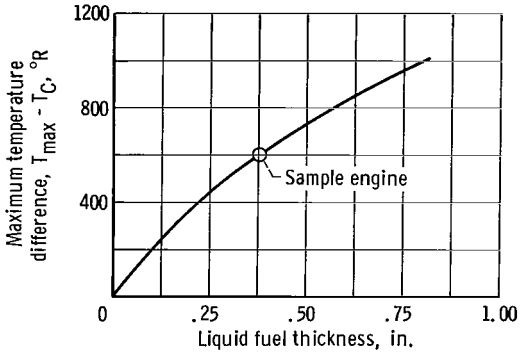

(b) Maximum temperature distribution.

Figure 24. - Effect of liquid fuel thickness on temperature distribution. Thermal conductivity of fuel, 300 Btu per hour per square foot per °F per inch; thermal conductivity of carbon, 26 Btu per hour per square foot per °R per inch.

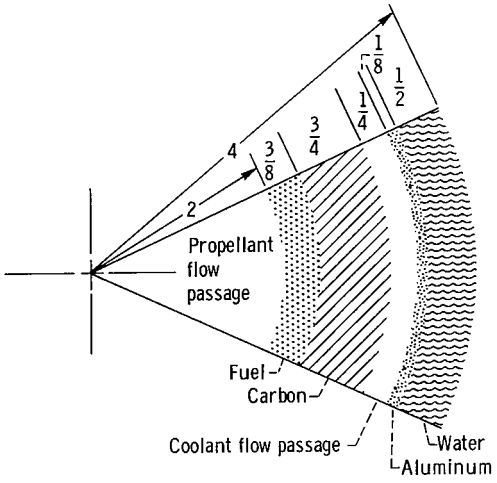

Figure 25. - Fuel element configuration used to estimate engine weight. (All dimensions are in inches.)

NASA-Langley, 1967 — 22 E-3743